Universidade de Lisboa

Faculdade de Medicina

THE ROLE OF N-TERMINAL PHOSPHORYLATION ON HUNTINGTIN

OLIGOMERIZATION, AGGREGATION AND TOXICITY

Joana Margarida Marques Branco dos Santos

Mestrado em Neurociências

2012

Universidade de Lisboa

Faculdade de Medicina

THE ROLE OF N-TERMINAL PHOSPHORYLATION ON HUNTINGTIN

OLIGOMERIZATION, AGGREGATION AND TOXICITY

Joana Margarida Marques Branco dos Santos

Mestrado em Neurociências, 2012

Dissertação orientada por:
Prof. Doutor Tiago F. Outeiro
Doutor Federico Herrera

A realização desta dissertação foi aprovada pela Comissão Coordenadora do Conselho Científico da Faculdade de Medicina da Universidade de Lisboa, em reunião de 28 de Fevereiro de 2012.

Acknowledgements

I would like, in this simple gesture, to mention and thank all of those involved in the development of this thesis:

To my supervisor Dr. Tiago Outeiro for the opportunity and support throughout this thesis.

To my co-supervisor Dr. Federico Herrera for the dedication, patience and great incentive for the development of this project. Thank you for all the dedicated time, help, transmission of knowledge and scientific discussions, and especially for the personal and scientific growth they provided me.

To the UNCM team for all the help and constructive critiques throughout this work, and for the interesting and exciting meetings that greatly contributed to the development of my scientific critical spirit. Special thanks to Susana Gonçalves for the help with microcopy and for all the good times, to Leonor Fleming for the help with Western blotting procedures, and to Teresa Pais for the help with flow cytometry results.

To Dr. Ana Sebastião for the dedication and passion to the Neuroscience Master course and practical solutions along these two years.

To António Temudo and José Rino for all the technical support with microscopy.

To the Flow Cytometry unit for all the help with the LSR Fortessa equipment.

Last but not least, to my family and friends for supporting me in all stages of my life. Without them, this thesis and the discoveries to come would not be possible.

Abstract

Huntington's disease (HD) is a hereditary disorder caused by a mutation in the exon-1 of the IT-15 gene, which encodes for a protein called huntingtin. The N-terminal region of mutant huntingtin is prone to aggregate and is toxic for specific types of neurons in the striatum and cortex, leading to the involuntary movements and psychiatric disturbances that characterize HD. Growing evidence indicates that the smaller, more soluble aggregates (dimers and oligomers) are the most toxic species, but little is still known about the process of huntingtin oligomerization.

The aim of this thesis was to elucidate the role of the N-terminal region of huntingtin on its oligomerization, aggregation and toxicity. We put special emphasis on its phosphorylatable residues (T3, S13 and S16), because phosphorylation pathways are involved in key aspects of HD. We used a huntingtin-Venus bimolecular fluorescence complementation (BiFC) assay recently developed in our laboratory. In this model, huntingtin exon-1 is fused to two non-fluorescent halves of the Venus protein (V1 and V2). When huntingtin dimerizes, the two halves get together and reconstitute the functional fluorophore. We used these BiFC constructs to create a series of phosphoresistant (T3A, S13A, S16A) and phosphomimic (T3D, S13D, S16D) huntingtin mutants and test their behavior in living cells. The presence of phosphomimic mutations in both 103QHtt-V1 and 103QHtt-V2 BiFC constructs completely abolished the generation of huntingtin aggregates. Combinations of a non-mutated construct with a phosphomimic construct produced intermediate phenotypes in terms of oligomerization and aggregation. Phosphoresistant BiFC pairs did not produce overt phenotypes. Mutations in N-terminal residues had varied effects on Htt toxicity, which apparently were not associated with the levels of oligomeric species or inclusion bodies.

Our results contribute to a better understanding of HD and highlight the therapeutic potential of targeting the phosphorylatable residues of N-terminal huntingtin.

Keywords: Huntington's disease; huntingtin; oligomeric species; phosphorylation; BiFC system.

Resumo

A doença de Huntington (HD) é uma doença hereditária causada por uma mutação no exão-1 do gene IT-15, que codifica para a proteína huntingtina. A região N-terminal da proteína mutada tem tendência para agregar e é tóxica para tipos específicos de neurónios no estriado e no córtex, levando ao aparecimento de movimentos involuntários e perturbações psiquiátricas, que caracterizam a doença. Evidências crescentes indicam que os agregados mais pequenos e solúveis (dímeros e oligomeros) representam as espécies mais tóxicas, no entanto, pouco se sabe acerca do processo de oligomerização da huntingtina.

O principal objectivo deste trabalho foi elucidar o papel da região N-terminal da huntingtina na sua oligomerização, agregação e toxicidade. Focámo-nos especialmente nos resíduos fosforiláveis (T3, S13 e S16), uma vez que as vias de fosforilação estão envolvidas em aspectos-chave da HD. Foi utilizado um sistema de complementação bimolecular de fluorescência(BiFC), recentemente desenvolvido no nosso laboratório. Neste modelo, o exão-1 da huntingtina é fundido com duas metades não fluorescentes da proteína Venus(V1 e V2). Quando a huntingina dimeriza, as duas metades unem-se, reconstituindo o fluoróforo funcional. Estas ferramentas BiFC foram utilizadas para criar vários mutantes resistentes à fosforilação (T3A, S13A, S16A) e constitutivamente fosforilados (T3D, S13D, S16D), sendo o seu comportamento testado em células vivas. Quando presentes em ambas as metades 103QHtt-V1 e 103QHtt-V2 BiFC, as mutações que imitam a fosforilação, resultaram na abolição de agregados nas células. Combinações de metades BiFC mutadas e não-mutadas produziram fenótipos mistos em termos de oligomerização e agregação. Mutantes BiFC resistentes à fosforilação não produziram fenótipos evidentes. As mutações nos resíduos da região N-terminal evidenciaram efeitos diversos na toxicidade da huntingtina, aparentemente não associados com os níveis de oligomeros ou agregados.

Os nossos resultados contribuem para uma melhor compreensão da HD, destacando o potencial alvo terapêutico dos resíduos fosforiláveis da região N-terminal da huntingtina.

Palavras-chave: Doença de Huntington; huntingtina; espécies oligoméricas; fosforilação; sistema BiFC.

General Contents

Index of Images

Index of Tables

List of abbreviations

Akt-1	Serine/threonine protein kinase B
Ala, A	Alanine
APP	Amyloid precursor protein
Asp, D	Asparagine
BACHD	HD mouse model based on bacterial artificial chromosome
BiFC	Bimolecular fluorescence complementation
CAG	Cytosine-adenine-guanine trinucleotide
Cdk5	Cyclin-dependent kinase 5
CK2	Casein kinase-2
CMV	Cytomegalovirus promoter
DRPLA	Dentatorubral-pallidoluysian atrophy
EDTA	Ethylenediaminetetraacetic acid
ER	Endoplasmic reticulum
FBS	Fetal bovine serum
GAC	Guanine-adenine-cytosine trinucleotide
GAPDH	Glyceraldehyde-3-phosphate dehydrogenase protein
GCC	Guanine-cytosine-cytosine trinucleotide
HD	Huntington's disease
Hsps	Heat-shock proteins
Htt	Huntintin protein
Httex1	Huntingtin exon 1
IKK	Ikappa B kinase
IT15	Interesting transcript 15 (gene)

LB	Luria Broth
LDH	Lactate dehydrogenase enzyme
NES	Nuclear export signal
NT17	N-terminal sequence of 17 amino acids
OH	Hydroxyl group
PAGE	Polyacrylamide gel electrophoresis
PBS	Phosphate buffer saline
PCR	Polymerase chain reaction
PolyA	Polyadenine
PolyQ	Polyglutamine
PRR	Proline-rich region
PVDF	Polyvinylidene difluoride
rpm	Revolutions per minute
SBMA	Spinal bulbar muscular atrophy
SCA	Spinocerebellar ataxias
SDS	Sodium dodecyl sulfate
Ser13, S13	Serine 13
Ser16, S16	Serine 16
SGK	Serum and glucocorticoid-induced kinase
TBS-T	Tris-HCl buffer saline-tween
Thr3, T3	Threonine 3
Tpr	Translocated promoter region
UPS	Ubiquitin–protease system
WT	Wild-type

1. Introduction

1.1. Huntington's Disease

Huntington's disease (HD) is a devastating neurodegenerative disorder first described by George Huntington in 1872 (Huntington, 1872). HD is caused by an abnormal expansion of a triplet cytosine-adenine-guanine (CAG) repeat in an autosomal dominant gene located in the short arm of chromosome 4. The worldwide prevalence is approximately 4 to 10 cases per 100,000 individuals, making it the most common inherited neurodegenerative disorder (Imarisio et al., 2008, Landles and Bates, 2004, Roos, 2010).

HD is characterized by motor, psychiatric and cognitive features. The first described symptom is known as chorea or jerky dance-like movements, and consists in involuntary movements of facial muscles and distal extremities that gradually extend to other skeletal muscles, ultimately affecting the motor control of all body, legs and arms. This inability to coordinate muscles is the result of a progressive cell loss in the striatum (caudate nucleus and putamen) of the basal ganglia, which primarily affects the medium spiny neurons (Figure 1). However, in late stages of the disease, neuronal degeneration extends to other areas of the brain, including thalamus and deep layers of the cortex. As a consequence, cognitive, behavioural and psychiatric complications emerge, including personality changes, irritability, anxiety, depression and dementia. Most HD patients also experience extreme weight loss and sleep disturbances (Costa et al., 2003, Kaplan and Stockwell, 2012, Mestre et al., 2009, Roos, 2010).

The gene responsible for HD, known as IT-15, is an extremely large 180 kb DNA sequence with 67 exons. The pathogenic CAG expansion is found in the first exon of the gene and encodes for an abnormally expanded polyglutamine (polyQ) amino acid sequence within the N-terminal region of the huntingtin protein (Htt) (Ambrose et al., 1994, The Huntington's

Disease Collaborative Research Group, 1993). In normal conditions, the number of CAG is repeated between 6 and 29 times. The disease manifests when this number increases over 36 repeats. Individuals with 29 to 36 CAG repeats are generally asymptomatic for the disease. However, these intermediate alleles are meiotically unstable and tend to expand above 36 repeats, causing the disorder in future generations especially when transmitted through the paternal line (Duyao et al., 1993, Trottier et al., 1994).

The length of expanded CAG is inversely correlated with the age of onset and directly correlated with the severity of the disease, i.e. the higher the number of CAG repeats, the earlier symptoms manifest and the more devastating is the disease. HD occurs most frequently in midlife, but the clinical symptoms can also appear in children or young adults. The juvenile cases of HD carry more than 55 CAG repeats and the disease progresses more rapidly, leading to death 11 years after its first manifestation, compared to 15-20 years of a typical adult onset (Foroud et al., 1999, Telenius et al., 1993).

Currently there are no drugs that can alter the course of HD, and available treatments act only at a symptomatic level. Additionally, many of the existent drugs have adverse side effects that can worsen HD pathology (Martin et al., 2008, Roos, 2010). Thus, a better understanding of HD pathogenesis is needed for the development of disease-modifying therapeutic strategies that can stop, delay or reverse the progression of HD.
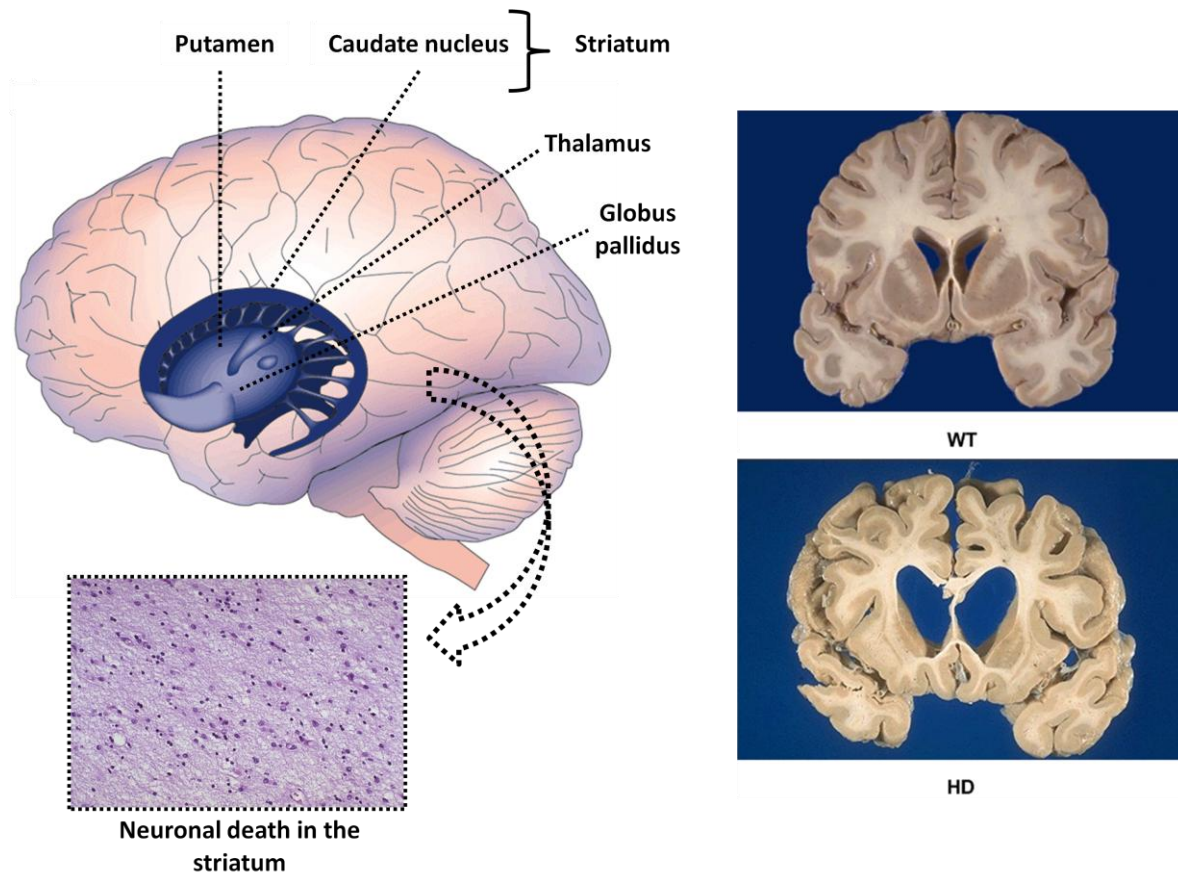
Figure 1. Selective neuronal degeneration in HD patient brains. The most common histopathological hallmark of HD is the accumulation of intracellular proteinaceous inclusions, which is associated with neurotoxicity in specific brain areas. Neuronal loss is primarily found in the neostriatum and cerebral cortex, many years before clinical symptoms appear, and marked striatal and cortical atrophy are already present at the time of diagnosis. Adapted from http://www.nature.com/nrm/journal/v1/n2/fig_tab/nrm1100_120a_F2.html http://medgen.genetics.utah.edu/photographs/pages/huntington.htm and http://marcora.caltech.edu/science.htm

1.2. Huntingtin protein and HD pathogenic mechanisms

Htt is an extremely large protein (350 kDa) that is ubiquitously expressed and widely distributed throughout all body tissues, included the brain (The Huntington's Disease Collaborative Research Group, 1993). The specific molecular role of normal Htt in neuronal and non-neuronal cell types is not well defined (Krobitsch and Kazantsev, 2011), but it plays a role as a scaffold protein in intracellular trafficking and signaling pathways (Rockabrand et al., 2007, Strehlow et al., 2007, Tukamoto et al., 1997). Htt is also associated with

transcription factors (Kegel et al., 2002, Zuccato et al., 2003) and implicated in synaptic (Smith et al., 2005) and anti-apoptotic processes (Leavitt et al., 2006, Luo and Rubinsztein, 2009). Additionally, Htt knockout mice are not viable and die as embryos, suggesting that wild-type (wt) Htt is essential for normal development (Duyao et al., 1995, Nasir et al., 1995, Zeitlin et al., 1995).

The expansion of the polyglutamine tract leads to both a gain of toxic function and a loss of normal Htt function (Cisbani and Cicchetti, 2012). Mutant Htt becomes involved in various aberrant protein-protein interactions that cause activation of pro-apoptotic proteins (Hermel et al., 2004, Yang et al., 2010), mitochondrial dysfunction (Orr et al., 2008, Panov et al., 2002), impaired vesicular trafficking (Gauthier et al., 2004, Qin et al., 2004), transcriptional dysregulation (Nucifora et al., 2001), excitotoxicity (Heng et al., 2009, Shin et al., 2005) and ultimately cell death (Zeron et al., 2001). The precise molecular mechanism of such pathological effects of mutant Htt is not clear. However, aberrant oligomerization of Htt molecules and their organization into amyloid-like proteinaceous aggregates is considered to have a leading role in HD pathogenesis. Htt aggregates are also the most common histopathological hallmark of the disease, being observed in neurons of all cortical layers and in medium-sized neurons of the striatum (Rochet, 2007). The presence of large amyloid inclusions is a feature shared by most neurodegenerative disorders, including many CAG repeat disorders such as spinocerebellar ataxias (SCA), spinal bulbar muscular atrophy (SBMA) and dentatorubral-pallidoluysian atrophy (DRPLA) (Kaplan and Stockwell, 2012, Martin et al., 2008).

The intracellular accumulation of mutant Htt is facilitated by its cleavage through caspase-mediated proteolytic degradation, which liberates toxic N-terminal fragments containing Htt exon 1 (Httex1) (Borrell-Pages et al., 2006). Expression of mutant Httex1 is

sufficient to cause the disorder in mice, strongly indicating that this fragment of the protein is a key player in HD pathogenesis (Mangiarini et al., 1996). Httex1-containing fragments are more prone to misfold and aggregate than full-length mutant Htt (Ross et al., 1999). The aggregation of proteolytic Htt fragments is a dynamic process that starts with the dimerization of soluble misfolded monomers and progresses towards the formation of small oligomers, ultimately leading to the production of larger and more insoluble structures, such as protofibrils, fibrils and inclusion bodies (Agorogiannis et al., 2004, Hartl and Hayer-Hartl, 2009, Zheng and Diamond, 2012, Zuccato et al., 2010) (Figure 2).
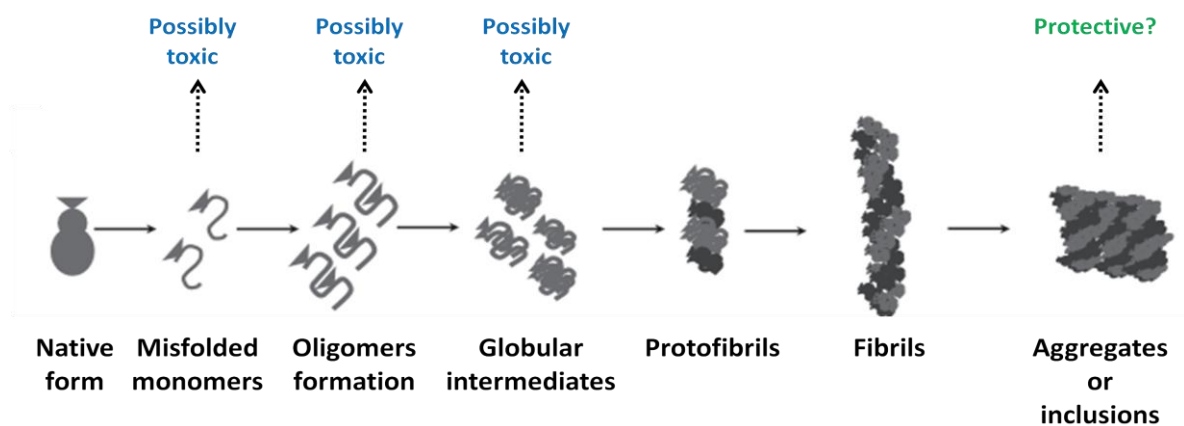
Figure 2. Aggregate formation process. Mutant Htt undergoes covalent modifications, such as cleavage or post-translational modifications, leading to conformational changes of the protein. The misfolded protein forms soluble oligomer intermediates that can accumulate as a globular structure and further form protofibrils. Protofibrils rearrange into amyloid-like structures, ultimately resulting in aggregates or inclusions. The aggregates consist of β-sheet-rich fibrils aligned side-by-side to form large insoluble species that were originally thought to be neurotoxic. However, several studies postulate that mutant Htt inclusions are not pathogenic but rather an attempt of the cells to sequester toxic soluble fragments. Adapted from (Zuccato et al., 2010).

Whether large, insoluble aggregates are toxic or protective species has been extensively debated. They were originally thought to be cytotoxic for several reasons. First, unlike soluble oligomers, they were clearly and easily observed in post-mortem histopathological studies of HD brains (Maat-Schieman et al., 1999, Sapp et al., 1997). Second, like the severity of the disease, the formation of large inclusion bodies is directly

correlated with polyglutamine repeat length both *in vitro* and *in vivo* and with worsening of HD clinical features (DiFiglia et al., 1997, Li and Li, 1998). A HD mouse model expressing mutant Httex1 showed a strong correlation between mutant Htt inclusions and disease progression. The formation of large inclusions was abolished when mutant Htt expression was blocked, leading to an amelioration of the behavioral phenotype (Yamamoto et al., 2000). And third, the accumulation of mutant Htt fragments has been associated with the failure of important cellular and molecular mechanisms for the maintenance of cell viability, such as ubiquitin–protease system (UPS) and the chaperone refolding cycles. Proteasome subunits and molecular chaperones were found within Htt aggregates, which suggests that misfolded Htt fragments are targeted for degradation but the UPS is unable to clear the large polyglutamine stretch, leading to its accumulation (Martin et al., 2008, Zuccato et al., 2010). Furthermore, overexpression of molecular chaperones, such as heat-shock proteins (Hsps) 70 and 104, has been shown to prevent the formation of large aggregates, to reduce cell death in mammalian cell models of HD and to increase life span in *Drosophila* and mouse models of the disease (Carmichael et al., 2000, Vacher et al., 2005, Warrick et al., 1999). However, these chaperones could reduce the number of large inclusions by preventing the formation of soluble intermediates, such oligomeric species, and/or by refolding smaller misfolded fragments (Imarisio et al., 2008). The same logic can be applied to the rest of the arguments in favor of the cytotoxicity of large protein inclusions, because they are always equally satisfactory if the toxic species were the oligomeric ones.

There is now increasing support for the idea that the formation of large aggregates are a protective cell mechanism to scavenge more soluble and toxic forms, such as dimers and oligomers (Arrasate et al., 2004, Bodner et al., 2006, Kuemmerle et al., 1999). Arrasate *et al.* (2004) showed that cells with large inclusions survived significantly longer than cells with

diffuse mutant Htt. Similarly, an *in vivo* study demonstrated that despite the presence of large inclusions in HD mouse brain expressing N-terminal fragments of Htt under the control of the endogenous human promoter (shortstop), no clinical evidence of neurodegeneration was observed (Slow et al., 2005). In the context of other neurodegenerative disorders, such as Parkinson's and Alzheimer's disease, oligomers are proven to be the most toxic species due to their higher reactivity and their ability to move more freely between cell and tissue compartments (Agorogiannis et al., 2004, Taylor et al., 2002). Most research has focused on the mechanisms of generation of large aggregates, mainly because they are obvious structures in cells and tissues. However, little is known about how smaller intermediate species, such as dimers and oligomers, are generated in HD. This is due, at least in part, to the lack of suitable experimental models for their visualization and study in living cells until relatively recently (Herrera et al., 2011, Lajoie and Snapp, 2010, Outeiro et al., 2008).

As mentioned above, the generation of N-terminal fragments containing Httex1 is a key step in HD pathology, Httex1 being sufficient to cause HD in animal models (Bates et al., 1998, Mangiarini et al., 1996). Httex1 contains an N-terminal sequence of 17 amino acids (NT17 domain) preceding the polyQ tract and a proline-rich region (PRR) (Figure 3). The first 17 amino acids of Htt are highly conserved throughout mammalian evolution, suggesting an important function of the NT17 domain (Atwal et al., 2007, Rockabrand et al., 2007). This domain contains a functionally active nuclear export signal (NES) that is responsible for the cytosolic localization of Htt, and the expansion of polyglutamine repeat or the removal of these amino acids lead to Htt nuclear accumulation (Cornett et al., 2005, Xia et al., 2003). Cornett *et al.* (2005) showed that the NT17 sequence binds to the nuclear pore protein Tpr, which exports proteins from the nucleus. Furthermore, the NT17 domain forms an amphipathic alpha helical membrane-binding domain that can reversibly target Htt to

mitochondria, endosomes and autophagic vesicules, Golgi apparatus and endoplasmic reticulum (ER) (Atwal et al., 2007, Rockabrand et al., 2007). This domain also plays an important role in mutant Htt aggregation, since it can interact with the adjacent polyQ region, influencing each other's structure and the aggregation properties of mutant Htt (Thakur et al., 2009, Williamson et al., 2010). Moreover, deletion or particular post-translational modifications of NT17, such as SUMOylation (Steffan et al., 2004), ubiquitination (Jana et al., 2005, Zucchelli et al., 2011), acetylation (Steffan et al., 2001) and phosphorylation (Aiken et al., 2009, Gu et al., 2009, Thompson et al., 2009), modulate the propensity of mutant Htt to form aggregates and its subcellular localization, clearance and toxicity.

The PRR, directly following the polyQ region, is a sequence of approximately 50 amino acids that comprises a stretch of 11 consecutive proline residues, followed by several mixed proline/glutamine residues with 7 scattered proline residues, and then another proline-enriched tract containing 10 consecutive prolines (Kaplan and Stockwell, 2012, Neveklovska et al., 2012). PRR can stabilize the structure of the polyQ stretch and is proposed to be involved in the interaction of Htt with several partners (Borrell-Pages et al., 2006, Kaplan and Stockwell, 2012). However, it does not seem to have a direct role in HD pathology. A very recent *in vivo* study showed that mice expressing huntingtin without PRR are born at normal frequency and develop normal motor function, coordination and balance, which suggests that PRR is not required for normal Htt function (Neveklovska et al., 2012).

1.3. Phosphorylation pathways involved in HD pathogenesis

The reversible addition of a phosphate group to amino acids containing an extra carboxyl residue (Serine, Threonine and Tyrosine) by kinases, or the inverse reaction catalyzed by phosphatases, can modulate the function of proteins. Concatenated

phosphorylation/dephosphorylation reactions are an important intracellular signaling mechanism that can turn on and off many biological processes, such as cell differentiation, proliferation and survival (Ehrnhoefer et al., 2011, Wang et al., 2010).

Phosphorylation pathways also play a significant role in mutant Htt cleavage, aggregation and toxicity. Htt can be phosphorylated at serine 421 by protein kinase Akt-1 and by the serum and glucocorticoid-induced kinase, SGK (Humbert et al., 2002, Rangone et al., 2004). Akt-1-mediated phosphorylation reduces caspase cleavage of mutant Htt, leading to a decreased formation of large inclusions and lower toxicity in HD models, both *in vitro* and *in vivo* (Humbert et al., 2002, Pardo et al., 2006, Warby et al., 2009), while SGK inhibits mutant Htt toxicity in striatal neurons (Rangone et al., 2004). Another crucial kinase involved in HD pathogenesis is the cyclin-dependent kinase 5 (Cdk5), which can reversibly interact with serines 434, 1181, 1201 (Anne et al., 2007, Luo et al., 2005). Phosphorylation of Htt at serine 434 has been shown to reduce Htt cleavage by caspase 3 at residue 513 and to attenuate aggregation (Luo et al., 2005). Constitutive phosphorylation of all three Cdk5 sites confers neuroprotective properties against mutant Htt toxicity (Anne et al., 2007, Luo et al., 2005).
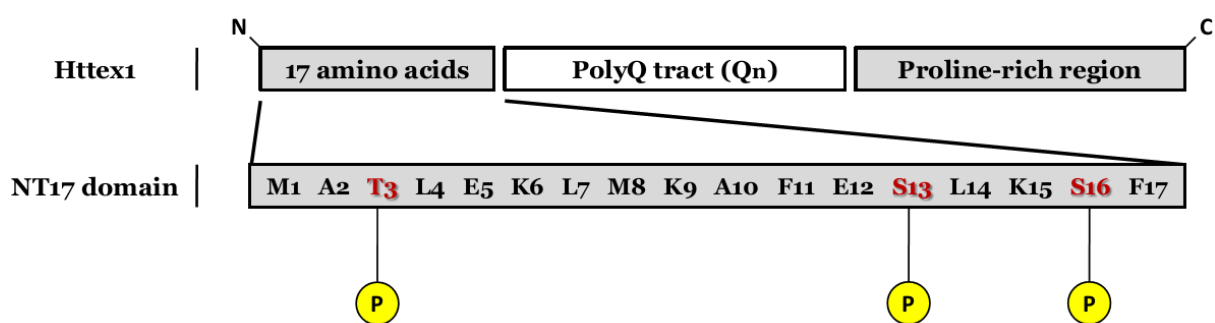
Figure 3. Structure of Huntingtin exon 1 and its phosphorylation sites. Httex1 contains an N-terminal region of 17 amino acids (NT17 domain) preceding a polyglutamine (PolyQ) tract and a Proline-rich region of 50 amino acids (PRR) on the C-terminal side of the polyglutamine tract. The NT17 domain can be phosphorylated at threonine (T) or serine residues (S), as indicated in yellow.

The NT17 domain has three sites that can be modified by phosphorylation: threonine 3 (Thr3 or T3), serine 13 (Ser13 or S13) and serine 16 (Ser16 or S16) (Figure 3). Aiken *et al*.

(2009) showed that the phosphorylation of Thr3 occurs *in vivo* and affects the behavior of mutant Htt. Mimicking Thr3 phosphorylation alters Htt aggregation, enhancing its propensity to form aggregates in striatal progenitor cells and increasing the levels of insoluble Htt species in a *Drosophila* HD model. In contrast, phosphorylation resistant mutants show a slight decrease in aggregation propensity, whereas both phosphomimic and phosphoresistant Thr3 mutations significantly reduce the neurodegeneration caused by mutant Htt *in vivo* (Aiken et al., 2009). Phosphorylation at Ser13 and Ser16 dramatically decreases Htt inclusion formation in a mammalian cellular model of the disease, and affects the alpha-helical conformation of the NT17 domain, targeting Htt to the nucleus (Atwal et al., 2011). Similarly, another study indicates that a constitutively phosphorylated state of Ser16 promotes the nuclear accumulation of Htt N-terminal fragments and reduces their affinity for the nuclear pore complex Tpr (Havel et al., 2011). Casein kinase-2 (CK2) inhibitors can reduce NT17 phosphorylation and result in greater mutant Htt toxicity, suggesting a protective role of Ser13 and Ser16 phosphorylation (Atwal et al., 2011). IKK, a kinase involved in inflammatory response, directly phosphorylates Htt at Ser13 and activates Htt clearance through proteosomal and lysosomal degradation mechanisms. Furthermore, the phosphorylation of Ser16 is facilitated by previous phosphorylation of Ser13 by IKK (Thompson et al., 2009). To address the importance of Ser13 and Ser16 phosphorylation *in vivo*, Gu *et al*. (2009) developed BACHD mice expressing Ser13 and Ser16 phosphomimic and phosphoresistant mutant Htt. Behavioral features of the disease, including motor and psychiatric deficits, are abolished when both serines are mutated to a phosphomimic residue. Moreover, mice expressing phosphomimic Ser13/Ser16 mutations show an impressive phenotype without aggregates in striatum and cortical layers of the brain, and have a later onset for

neurodegenerative events. Phosphoresistant mutants do not show any effect on behavior or histopathology of HD mice (Gu et al., 2009).

Since the NT17 domain plays a key role in HD pathogenesis, understanding the phosphorylation pathways involved in the post-translational modification of these residues could provide insight into novel strategies for HD treatment. However, how NT17 is phosphorylated and how this event regulates Htt oligomerization and toxicity remain poorly understood.

1.4. Bimolecular fluorescence complementation (BiFC) as a model for the study of Htt oligomerization in living cells

Most proteins can be split in two fragments that do not retain the original activity of the protein but can recover it when they are brought together in certain conditions (Kerppola, 2008). This property of proteins is called protein complementation, and it is widely used for biological assays since its discovery in 1958 (Richards, 1958). A complementation assay with a fluorescent protein, the green fluorescent protein (GFP), was first developed for the study of protein-protein interactions in bacteria (Ghosh et al., 2000). Two years later, fluorescence complementation was implemented for the analysis of protein-protein interactions in mammalian cells, and the method was named bimolecular fluorescence complementation (BiFC) assay (Hu et al., 2002). Since then, BiFC has been used in several model organisms, enabling the direct visualization of protein interactions in living cells and providing a powerful technique for genetic or pharmacological screens. This assay is based on the formation of a fluorescence complex when two proteins of interest, fused to non-fluorescent fragments of a reporter protein, interact with each other and reconstitute the activity of the reporter protein (Herrera et al., 2012, Goncalves et al., 2010).

The BiFC system has also proven to be a useful tool for the study of aberrant protein dimerization and oligomerization in the context of neurodegenerative disorders. We and others have recently developed BiFC models for the visualization and study of toxic misfolding proteins in living cells, including alpha-synuclein (Outeiro et al., 2008), huntingtin (Herrera et al., 2011, Lajoie and Snapp, 2010), APP (Chen et al., 2006) and tau protein (Chun et al., 2011). The system developed by Herrera *et al.* (2011) is based on the fusion of Httex1 to two non-fluorescent halves of the Venus fluorescent protein, a third generation variant of the yellow fluorescent protein YFP. When huntingtin dimerizes, the Venus halves are brought together and reconstitute the functional fluorophore (Figure 4A). Fluorescence is then directly proportional to the amount of oligomeric species within cells, and can be measured by conventional methods, such as flow cytometry or microscopy. Herrera et al. (2011) showed that Htt monomers, oligomeric species and large inclusions are visually distinguishable in living mammalian cells. Monomeric species do not produce fluorescence, whereas oligomers are observed as a homogeneously distributed fluorescence and large inclusions as localized foci of intense fluorescence (Herrera et al., 2011) (Figure 4B). Dimers and oligomers are indistinguishable by this method and we will refer to both as oligomeric species throughout the thesis. Moreover, this system allows the quantification of cell-to-cell transmission of mutant Htt by flow cytometry (Herrera et al., 2011), and the identification of molecular modifiers of Htt aggregation (Herrera and Outeiro, 2012). In summary, these data indicate that the Htt BiFC system is a promising tool for the search of novel molecular targets for HD therapeutics and other neurodegenerative disorders involving protein misfolding and aggregation.
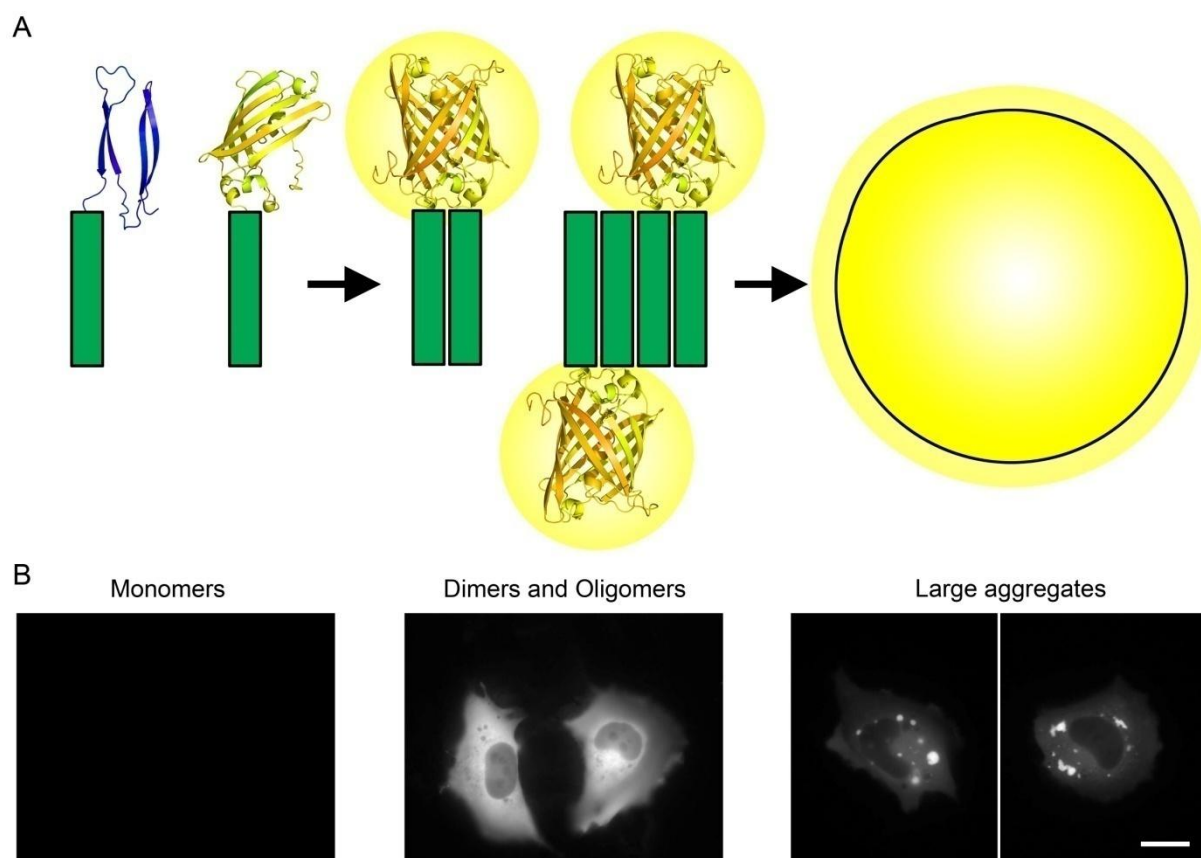
Figure 4. Schematic representation of the BiFC cellular model used for the visualization of mutant Httex1 oligomeric species in living mammalian cells. (**A**) Httex1 is fused to two non-fluorescent halves of the Venus fluorescent protein. When Htt dimerizes, the Venus halves are brought together and reconstitute the functional fluorophore, emitting fluorescence that can be easily measured by conventional methods. **(B)** In this model, monomers do not show fluorescence; dimers and oligomers show a homogeneously distributed fluorescence in the subcellular compartment where they are formed; and larger inclusions are observed as brighter regions with different morphologies that "scavenge" fluorescence from the rest of the cell. Scale bar, 20 μm.

2. Objectives

The main goal of this study is to understand how NT17 phosphorylation regulates the oligomerization, aggregation and toxicity of mutant Htt. In order to address this question, we used the Httex1-Venus BiFC system recently developed in our laboratory (Herrera and Outeiro, 2012, Herrera et al., 2011) to produce a series of point mutants of the NT17 domain. These mutations affect the phosphorylatable residues of this domain (Thr3, Ser13 and Ser16) and mimic the phosphorylation and dephosphorylation of such residues. The oligomerization, aggregation and toxicity of phosphomutant constructs will be then compared to their non-mutated counterpart.

3. Methods

3.1. Generation of NT17 phosphomutants from Htt-Venus BiFC constructs

The Htt-Venus BiFC cellular model recently developed in our group was used as a starting point for the production of the NT17 phosphomutant constructs mentioned above. We generated six different phosphomutant (phosphomimic and phosphoresistant mutants) constructs using the original 103QHtt-Venus1 and 103QHtt-Venus2 BiFC plasmids as a template (Figure 5). For the sake of simplicity, we will refer to both 103QHtt-Venus1 and 103QHtt-Venus2 BiFC plasmids as 103QHtt-Venus BiFC constructs throughout the present thesis. These constructs encoded for Htt exon1 fused to two non-fluorescent halves of the Venus fluorescent protein (Venus 1, amino acids 1-158, and Venus 2, amino acids 159-238). Venus halves are located in the C-terminal part of Htt exon1, a location that was found optimal in previous work from our laboratory (Herrera et al., 2011). The expression of the fusion proteins is constitutively regulated by the cytomegalovirus promoter (CMV), which induces high levels of expression. A bovine growth hormone polyA sequence is located after the Htt-Venus fusion proteins for mammalian expression. The polyglutamine region of Htt contains 103 glutamines, a tract length that is correlated with early-onset, extremely severe cases of HD. 103QHtt-Venus BiFC constructs also contain ampicillin- and neomycin-resistance sequences in order to select those bacteria or mammalian cells that carry the constructs.
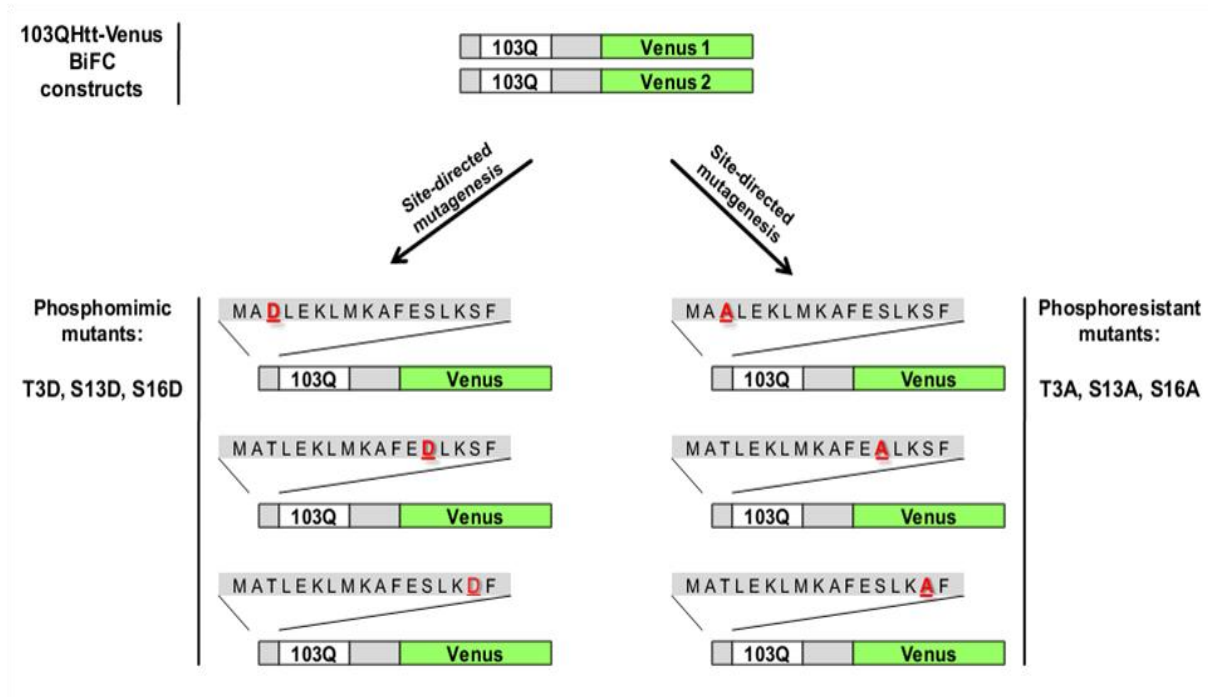
Figure 5. Schematic representation of the phosphomimic and phosphoresistant mutants. To evaluate the role of T3, S13 and S16 phosphorylation in mammalian cells, these residues were mutated to aspartate (T3D, S13D, S16D) or alanine (T3A, S13A, S16A). Aspartate mimics phosphorylated residues and alanine is not phosphorylatable, mimicking a constitutively unphosphorylated residue.

Single point mutations were independently induced in the three phosphorylatable residues (Threonine 3, Serine 13 and Serine 16) within the N-terminus of 103QHtt-Venus BiFC plasmids. The substitution of these phosphorylatable residues to Alanine (Ala, A) or Asparagine (Asp, D) confers them phosphoresistant or phosphomimic properties, respectively (Aiken et al., 2009, Gu et al., 2009). The negative charge of aspartic acid resembles phosphorylation, mimicking a constitutively phosphorylated state. On the other hand, the absence of the hydroxyl group (OH-) in alanine makes it virtually impossible to phosphorylate the residue, mimicking a constitutively unphosphorylated state. The general procedure for the generation of the phosphomutant constructs is explained below and illustrated in the following workflow (Figure 6).
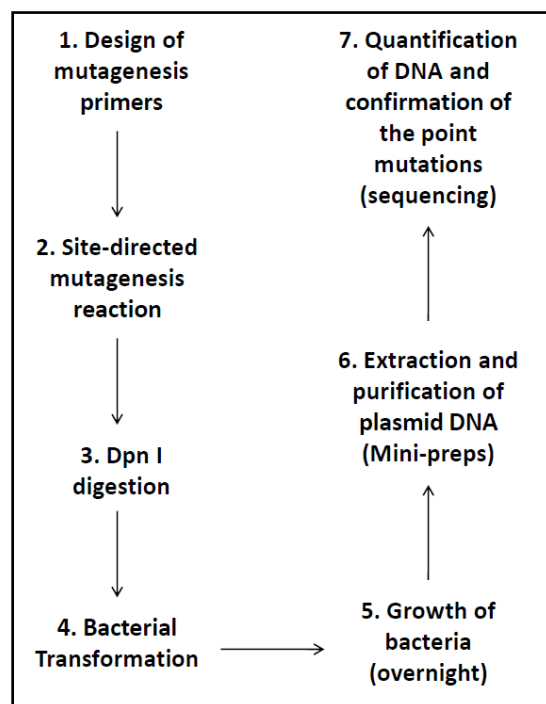
Figure 6. Workflow for the generation of NT17 phosphomutant constructs.

3.1.1. Design of mutagenesis primers

Eight pairs of mutagenesis primers (8 forward and 8 reverse) were designed by means of the PrimerX free software (http://www.bioinformatics.org/primerx/) (Table I). The original codons corresponding to phosphorylatable amino acids (Thr3, Ser13, Ser16) were replaced by GCC or GAC mutant codons, which encode for Alanine (Ala, A) or Asparagine (Asp, D), respectively (Figure 7).

Figure 7. Selected mutant triplets for the production of phosphoresistant or phosphomimic mutations. To induce the single point mutations in the phosphorylatable residues Thr3, Ser13 and Ser16, their original codons (ACC, TCC, AGC) were substituted by selected codons that encode for the amino acids Ala (GCC) or Asp (GAC).

3.1.2. Site-directed mutagenesis

PCR-based site-directed mutagenesis was used to produce the NT17 phosphomutants from the 103QHtt-Venus BiFC templates. Briefly, a PCR was carried out using the *PfuTurbo®* DNA *Polymerase* (Stratagene, La Jolla, CA, USA) (1.25 U), the 103QHtt-Venus BiFC templates (10 ng) and the mutagenesis primers (62.5 ng, each primer), and the following conditions: 1 min at 95ºC, 18 cycles x [50 s at 95ºC, 50 s at 60ºC, 8 min at 68ºC] and 10 min at 68ºC. The forward and reverse oligonucleotide primers used to introduce the specific point mutations are summarized in Table I.

Table I. Primers for site-directed mutagenesis. In red are represented the specific nucleotide mutation that will confer phosphoresistant properties to the residue, and in green, the selected nucleotide substitution for the generation of phosphomimic mutants.

Mutation	Htt-Venus BiFC plasmid template	Forward Primer	Reverse Primer
T3A	**Htt-Venus1**	5' ACCGCCATGGC**G**GCCCTGGAAAAGCTGATGAA 3'	5' TTCATCAGCTTTTCCAGGG**C**CGCCATGGCGGT 3'
	Htt-Venus2	5' ACTTAAGATGGCG**G**CCCTGGAAAAGCTG 3'	5' CAGCTTTTCCAGGG**C**CGCCATCTTAAGT 3'
S13A	**Htt-Venus1** **Htt-Venus2**	5' GAAGGCCTTCGAG**G**CCCTCAAAAGCT 3'	5' AGCTTTTGAGGG**C**CTCGAAGGCCTTC 3'
S16A	**Htt-Venus1** **Htt-Venus2**	5' CGAGTCCCTCAAA**GC**CTTCCAACAGCAGC 3'	5' GCTGCTGTTGGAAG**GC**TTTGAGGGACTCG 3'
T3D	**Htt-Venus1**	5' ACCGCCATGGCG**GA**CCTGGAAAAGCTGAT 3'	5' ATCAGCTTTTCCAGG**TC**CGCCATGGCGGT 3'
	Htt-Venus2	5' TTAAACTTAAGATGGCG**GA**CCTGGAAAAGCTGATGAA 3'	5' TTCATCAGCTTTTCCAGG**TC**CGCCATCTTAAGTTTAA 3'
S13D	**Htt-Venus1** **Htt-Venus2**	5' ATGAAGGCCTTCGAG**GA**CCTCAAAAGCTTCC 3'	5' GGAAGCTTTTGAGG**TC**CTCGAAGGCCTTCAT 3'
S16D	**Htt-Venus1** **Htt-Venus2**	5' TCGAGTCCCTCAAA**GA**CTTCCAACAGCAGCA 3'	5' TGCTGCTGTTGGAAG**TC**TTTGAGGGACTCGA 3'

3.1.3. DpnI digestion and Bacterial Transformation

The resulting mutagenesis reactions were incubated with DpnI (Promega, Madison, WI, USA) at 37°C, for 2 hours. The DpnI endonuclease cleaves specifically methylated and hemimethylated DNA. DNA isolated from most *E.coli* strains is methylated and therefore susceptible to DpnI digestion. However, the mutagenesis PCR product is the result of an *in vitro* synthesis reaction, and it has not been in contact with any type of methylase. As a consequence, it is not methylated and not susceptible to DpnI digestion. This property of DpnI allows for the selective digestion of the DNA template (methylated) and the selection of the mutated constructs synthesized de novo (not methylated). The digested DNA solutions that theoretically contain only the mutant plasmids were then transformed into thermocompetent

bacteria, following a Heat-Shock Long-Term protocol. The mutant plasmids were mixed with thawed competent bacteria and then incubated for 30 min on ice. Heat-shock of bacteria cells was performed by placing the tubes on a heat-block for 45 s, at 42°C. The tubes were then immediately placed on ice for 2 min, and the resulting solutions incubated in 300 μl of liquid Luria Broth (LB) 1X medium [1% w/v Tryptone; 0.5% w/v Yeast extract; 171 mM NaCl] without antibiotics for 1 hour at 37°C in agitation (200 rpm). The transformed bacteria were seeded on LB/Agar 1X [1% w/v Tryptone; 0.5% w/v Yeast extract; 171 mM NaCl; 1.5% w/v Agar] petri dishes containing 100 μg/ml of ampicillin as selection antibiotic and incubated overnight at 37°C.

3.1.4. Extraction and purification of DNA mutated plasmids

In order to obtain enough plasmid DNA for extraction and purification, clones were grown in agitation (200 rpm) in 4 ml of liquid LB 1X medium [1% w/v Tryptone; 0.5% w/v Yeast extract; 171 mM NaCl] containing 100 μg/ml of ampicillin at 37°C overnight. Plasmid DNA was then extracted by means of the Zyppy^{TM} Plasmid Miniprep Kit (Zymo Research, Irvine, CA, USA) following manufacturer's instructions.

3.1.5 Confirmation of the point mutations within NT17 domain

After extraction, DNA was quantified in a Nanodrop 2000 (Thermo Fisher Scientific Inc., West Palm Beach, FL, USA) and sequenced by means of external DNA sequencing services (Stabvida, Monte da Caparica, Setúbal, PT) to confirm the point mutations. The analysis of sequencing results was carried out by means of the Sequence Scanner Software v1.0 (Applied Biosystems, Life Technologies, Carlsbad, CA, USA) and the comparison of sequences was performed using the Basic Local Alignment Search Tool

(http://blast.ncbi.nlm.nih.gov/). Positive clones were stored as glycerol stocks at -80°C for future use.

3.2. Experiments in mammalian cells

The six phosphomutant constructs were tested for their behavior in cultured cells in comparison to the original, non-mutated (103Q) and to wt (25Q) Htt-Venus BiFC constructs (Figure 8). The experiments were carried out in Human H4 glioma cells, which were maintained and seeded in suitable culture conditions and transfected with the different combinations of plasmids. Twenty-four hours after transfection, the effect of the mutations on huntingtin's oligomerization and aggregation was evaluated by flow cytometry, fluorescence microscopy, native-PAGE immunoblotting and filter trap assays. The presence, number, morphology and size of Htt aggregates were quantified by microscopy. Finally, the toxicity of the different Htt versions was evaluated by means of the LDH release assay (Clontech Laboratories Inc., Mountain View, CA, USA).
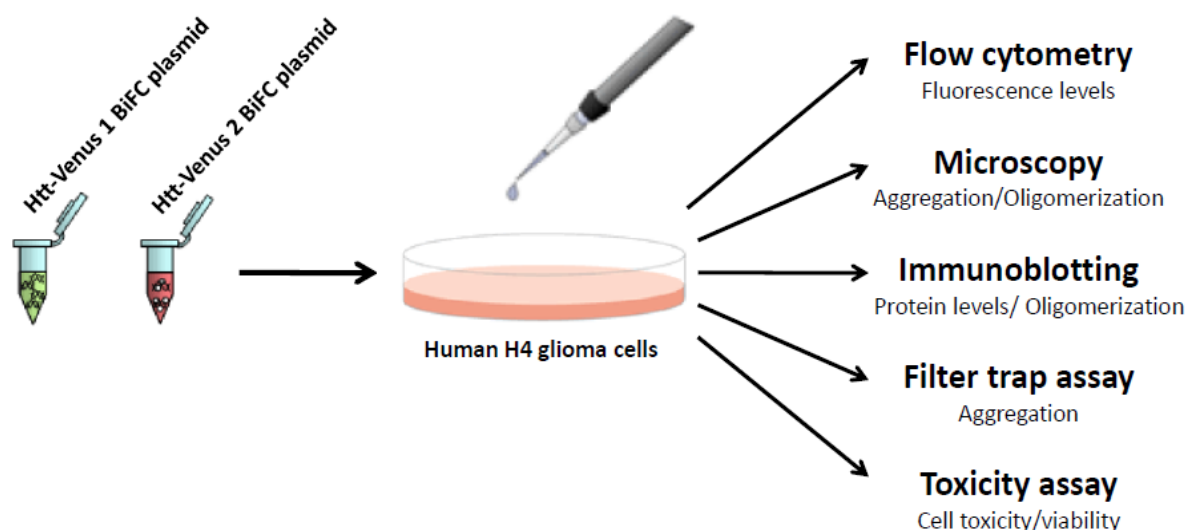
Figure 8. Testing the behavior of Htt-Venus BiFC mutant constructs in H4 cells. Cells were transfected with the phosphomutant (phosphomimic or phosphoresistant mutants), non-mutated (103QHtt-Venus) or wt (25QHtt-

Venus) BiFC pairs of plasmids. Twenty-four hours later, transfected cells expressing various Htt constructs were analyzed for fluorescence levels, aggregation, oligomerization and cell viability by means of several purpose-specific methods/techniques.

3.2.1. Cell Culture

Human H4 glioma cells (ATCC HTB-148, LGC Standards, Barcelona, Spain) were maintained in OPTI-MEM I (Gibco, Invitrogen, Barcelona, Spain) supplemented with 10% fetal bovine serum (FBS) and 1% of a penicillin/streptomycin commercial antibiotic mixture (Gibco, Invitrogen, Barcelona, Spain), under controlled conditions of temperature and CO_2 (37^oC, 5% CO_2). For all the experiments, cells were counted and seeded at a density of 10.000 cells/cm^2. Depending on the analytical method, cells were seeded on different types of plates. The density was maintained among the different sizes of plates in order to obtain comparable results with different techniques. For flow cytometry and toxicity assays, cells were grown on 6-well plates (35 mm per well diameter, Techno Plastic Cultures AG, Switzerland) and seeded in duplicate for each experimental group (2 wells per group). For microscopy, cells were seeded on glass- bottom 35 mm dishes (10 mm glass surface diameter, MatTek Corporation, Ashland, MA, USA). For protein extraction (PAGE and filter trap assays) cells were seeded in 100 mm dishes (Techno Plastic Cultures AG, Switzerland), respectively. Twenty-four hours later, X-tremeGene 9 DNA transfection reagent (Roche diagnostics, Mannheim, Germany) was used to transiently transfect cells with the different combinations of plasmids, according to the manufacturer's instructions. We and others have observed that 103QHtt expression is much less efficient than 25QHtt expression, resulting in impaired protein levels when cells are transfected with the same amount of plasmid. Such expression differences cause biased experimental results, 25QHtt being more toxic and producing more aggregates than 103QHtt. In order to correct this, 103QHtt-Venus (phosphomutants and non-mutated plasmids) and 25QHtt-Venus BiFC plasmids were used in an approximate proportion

of 1:6, as previously described (Herrera et al., 2011). Twenty-four hours after transfection, cells were handled according to the requirements of each analytical method.

3.2.2. Flow cytometry

The fluorescence intensity of transfected cells was determined by flow cytometry. Cells were washed once with phosphate buffer saline (PBS) [1 mM KH_2PO_4; 155 mM NaCl; 3 mM Na_2HPO_4-$7H_2O$; manufactured without Ca^{2+}, Mg^{2+} or phenolsulfonphthalein (PSP)] (Gibco, Invitrogen, Barcelona, Spain), trypsinized (0.05 % w/v, $37^{o}C$, 5 min) and collected into BD Falcon Round-Bottom Tubes (BD Biosciences, San Jose, CA, USA). Cells were then resuspended in PBS at room temperature and analyzed by means of a LSR Fortessa flow cytometer (Beckton Dickinson, Franklin Lakes, NJ, USA). Ten thousand cells were analyzed per experimental group. The FlowJo software (Tree Star Inc., Ashland, OR, USA) was used for data analysis and representation.

3.2.3. Microscopy and Image Analysis

All images of fluorescent living cells were acquired using an Axiovert 200M widefield fluorescence microscope equipped with a CCD camera (Carl Zeiss MicroImaging GmbH, Germany). Pictures of a total of 50-100 cells per experimental group were taken and then analyzed by means of the ImageJ free online software (http://rsbweb.nih.gov/ij/). The percentage of cells with aggregates was calculated by dividing the total number of cells with aggregates by the total number of transfected cells. The average number of aggregates per cell was calculated by dividing the total number of aggregates in all cells by the total number of cells with aggregates. The different types of aggregates were classified in three size categories (<1μm, 1-3μm, >3μm), and the percentage of aggregates from each category was calculated

by dividing the total number of aggregates of the category by the total number of aggregates of any size. All graphics were made by means of the GraphPad Prism 5 software (GraphPad Software Inc., La Jolla, CA, USA).

3.2.4. Protein extraction

For protein extraction, cells were washed once with PBS, lysed with a lysis buffer and scrapped directly from the plates. For denaturalizing conditions, cells were incubated with a triton-based lysis buffer (1% Triton X-100, 150 mM NaCl, 50 mM Tris pH 7.4) and a protease inhibitor cocktail tablet (Roche diagnostics, Mannheim, Germany). For native conditions, cells were incubated with a lysis buffer without denaturing detergents (173 mM NaCl, 50 mM Tris pH 7.4, 5 mM EDTA) and a protease inhibitor cocktail tablet (Roche diagnostics, Mannheim, Germany). In order to avoid protein degradation, cells were always kept on ice during the extraction procedure. The Soniprep 150 sonicator (Albra, Milano, Italy) was used to sonicate cells for 10 sec at 5 mA. Sonication was essential to disrupt membranes and to release proteins from the cellular pellet, allowing their subsequent isolation and detection by western blotting. Cells were then centrifuged at 10,000 x g for 10 min at 4°C and the supernatant containing the proteins was collected. Protein concentration was quantified by means of the BCA Protein Assay Reagent Kit (Thermo Fisher Scientific Inc., Rockford, IL, USA), following manufacturer's instructions.

3.2.5. Immunoblotting

Equals amounts of protein (15 μg) from each extract were prepared for analysis by western blotting under denaturing and native conditions. For denaturing conditions, loading buffer (200 mM Tris-HCl pH 6.8; 8% SDS; 40% glycerol; 6.3% β-mercaptoethanol; 0.4%

bromophenol blue) was added to the samples, which were then boiled for 5 min at 95°C and resolved on 12% SDS-polyacrylamide gel electrophoresis with SDS-containing running. For native conditions, SDS- and mercaptoethanol-free loading buffer (200 mM Tris-HCl pH 6.8; 40% glycerol; 0.4% bromophenol blue) was added to the samples, and the boiling step was omitted. Samples were directly loaded and run on 5% Native (SDS-free)-polyacrylamide gels using SDS-free running buffer. Protein transfer to PVDF membranes was carried out by means of the Trans-Blot Turbo^{TM} Transfer Starter System (Bio-rad, Hercules, CA, USA). After transfer, Ponceau S staining was performed on membranes to verify protein transfer efficiency as well as equal sample loading.

Membranes were blocked with 5% non-fat dry milk in Tris-HCl buffer saline-Tween (TBS-T) (150 mM NaCl, 50 mM Tris pH 7.4, 0.5% Tween-20) for 1 hour at room temperature in agitation. Membranes were incubated with a mouse monoclonal Htt antibody (1:500, Millipore, Billerica, MA, USA) overnight at 4°C in agitation; or with a mouse monoclonal GAPDH antibody (1:30000, Ambion, Austin, TX, USA) for 1 hour at room temperature in agitation. The primary antibodies were previously diluted in 5% bovine serum albumin (BSA) in TBS 1X (150 mM NaCl, 50 mM Tris pH 7.4) and 0.05% of sodium azide. Membranes were then washed 3 times in TBS-T and incubated with a secondary mouse IgG Horseradish Peroxidase-linked antibody (GE Healthcare Life Sciences, Uppsala, Sweden), previously diluted in 5% non-fat dry milk in TBS-T, under the following conditions: 1:5000 for 2-3 hours (for Htt) or 1:40000 for 30 min (for GAPDH) at room temperature in agitation. Membranes were washed 3 times in TBS-T and the immunoblot signal was developed by enhanced chemiluminescence reagents (Millipore, Billerica, MA, USA) and exposition to autorradiographic films.

3.2.6. Filter trap assay

Protein extracts were obtained in native conditions, as described above, and SDS was added to 100 µg of each extract to a final SDS concentration of 0.4% (w/v). The samples were passed through cellulose acetate membranes (0.22 µm pore; GE Water & Process Technologies, Fairfield, CT, USA) by vacuum, using a dot blot device. Cellulose acetate membranes were previously incubated with PBS 1X and 1% (w/v) SDS solution. After filtration, wells were washed twice with PBS 1X and 1% (w/v) SDS solution, and membranes were then blocked, incubated with antibodies and submitted to chemiluminescence detection as described above.

3.2.7. Toxicity assay

A colorimetric LDH release assay was used to measure the toxicity levels of the different constructs. This assay is based on the measurement of the activity of lactate dehydrogenase (LDH), a cytosolic enzyme that is released to extracellular medium upon damage to the cell membrane. Therefore, extracellular levels of LDH are directly proportional to cell toxicity. Cells were plated in duplicate for each experimental group (2 wells of 6-well plates) and transfected with the different combinations of plasmids. Twenty-four hours after transfection, 5µl of medium were collected in triplicate from each well into a 96-well plate (Techno Plastic Cultures AG, Switzerland) and the LDH activity determined by means of the LDH cytotoxicity detection kit (Clontech Laboratories Inc., Mountain View, CA, USA) following manufacturer's instructions. The absorbance of the samples was read at 492 nm using the Infinite M200 plate reader (Tecan, Männedorf, Switzerland). The average absorbance value was calculated and released LDH activity was graphically represented in

arbitrary units using the GraphPad Prism 5 software (GraphPad Software Inc., La Jolla, CA, USA).

3.2.8. Statistics

GraphPad Prism 5 software (GraphPad Software Inc., La Jolla, CA, USA) was used to perform the statistical analysis. Results are shown as the average ± standard deviation of at least 3 independent experiments. Results were analyzed by means of a one-way ANOVA followed by a Tukey's Multiple Comparison Test for comparison of averages. Results were considered significant only when $p < 0.05$.

4. Results

4.1. NT17 phosphomimic mutations affect mutant huntingtin oligomerization and aggregation

NT17 phosphorylation has been shown to modulate the aggregation and toxicity of mutant Htt (Aiken et al., 2009, Gu et al., 2009, Thompson et al., 2009). To elucidate the effect of NT17 phosphorylation in the oligomerization, aggregation and toxicity of mutant Htt in living mammalian cells, a series of 103QHtt-Venus BiFC phosphomutant constructs were generated as described in the Material and Methods section (Figure 5). The aggregation pattern of phosphomimic (T3D, S13D, S16D) and phosphoresistant (T3A, S13A, S16A) mutants was compared with non-mutated 103QHtt BiFC (103Q wt) constructs. The non-mutated 103QHtt BiFC pair showed both cytosolic homogenous fluorescence (oligomers) and large intracellular fluorescent aggregates (inclusion bodies) (Figure 9A), confirming previous reports (Herrera and Outeiro, 2012, Herrera et al., 2011). Surprisingly, all cells expressing NT17 phosphomimic constructs showed a striking phenotype without aggregates, and the presence of large aggregates was completely displaced by a homogeneous cytosolic fluorescence (Figure 9A). These results strongly suggest that NT17 phosphorylation totally abolishes the formation of large Htt aggregates and favors the production of more soluble dimers and oligomeric species. Phosphoresistant BiFC pairs showed a phenotype very similar to non-mutant 103QHtt, having both diffuse fluorescence and large aggregates in the cytoplasm (Figure 9A). Consistently, no significant differences were observed in terms of number and size of Htt aggregates (Figure 9C-E). However, when cells were transfected with the S16A 103QHtt BiFC pair constructs, the percentage of cells with large aggregates increased slightly but significantly (Figure 9B). This result could indicate that the dephosphorylation of Serine16 increases the propensity of mutant Htt to form large

aggregates inside the cells. In fact, there was a tendency, not reaching statistical significance, of all phosphoresistant mutants to increase the number of aggregates per cell (Figure 9C and 9D). The size of the aggregates did not change (Figure 9E).

A

B

C

D

E
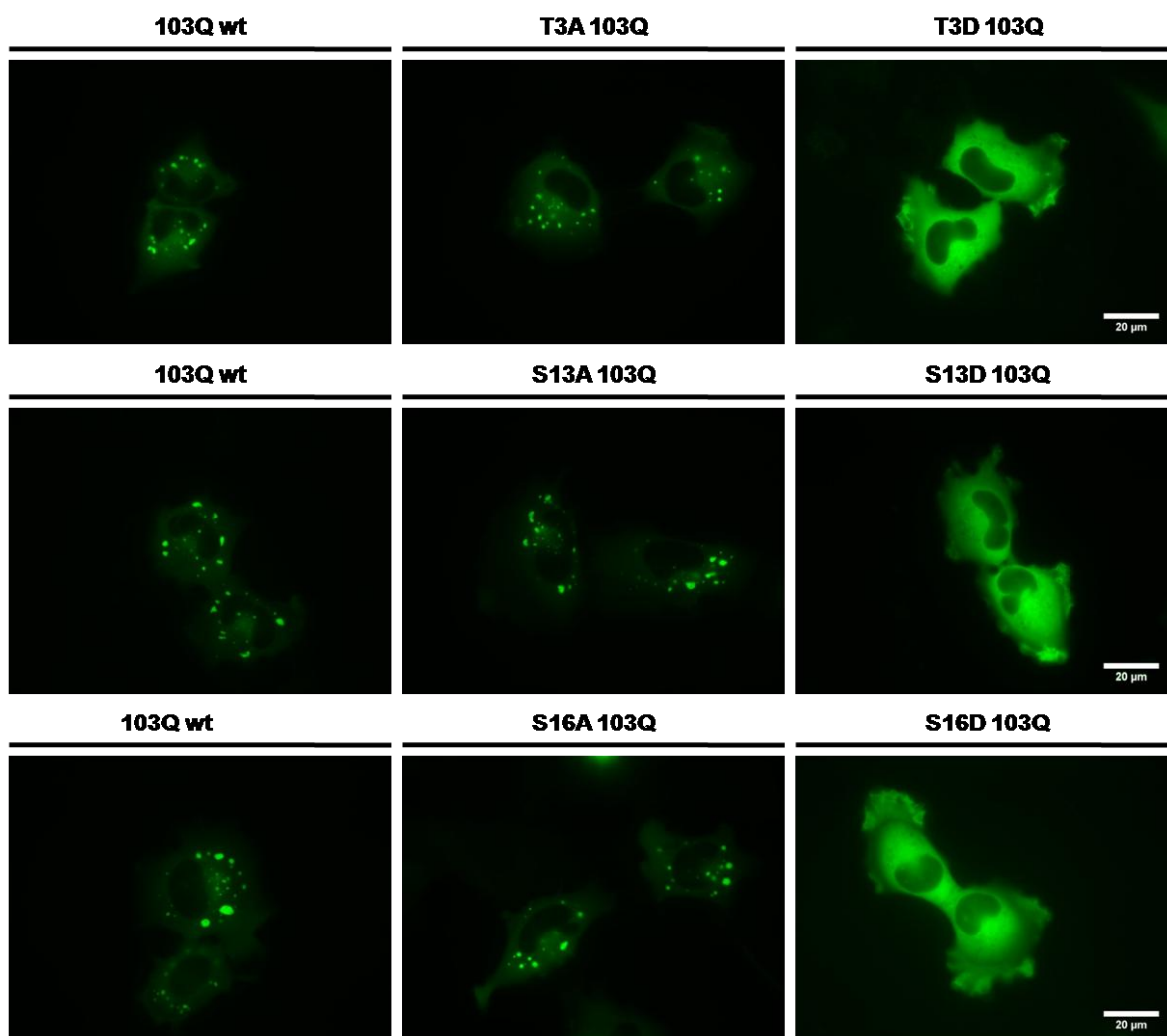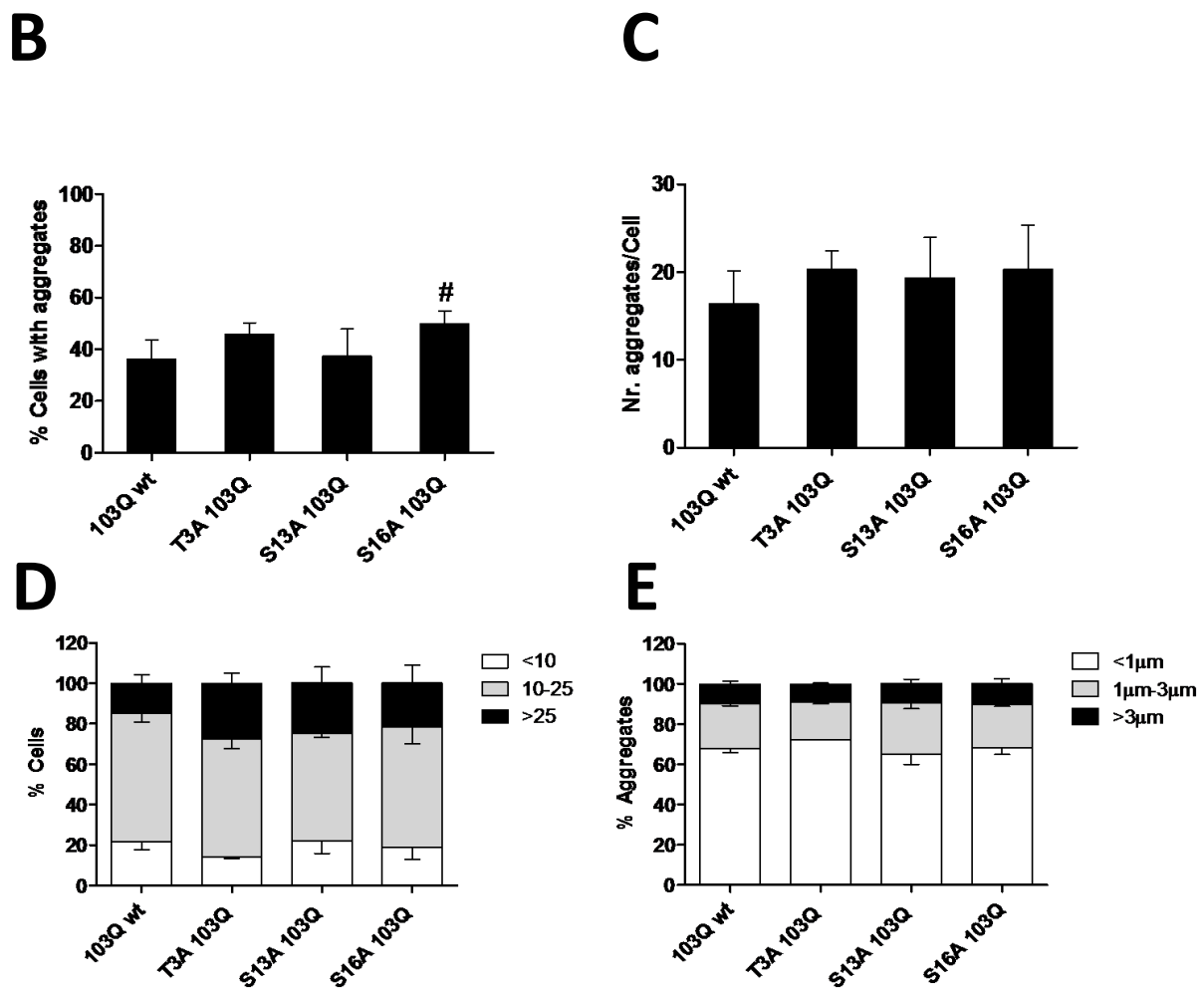
Figure 9. Phosphorylation of NT17 residues abolishes the accumulation of large Htt aggregates in H4 cells. **(A)** Cells were transfected with the indicated pairs of BiFC constructs, and the generation of large aggregates was evaluated by means of fluorescence microscopy. The 103QHtt pair of constructs typically shows large aggregates in the cytosol. While the phenotype of phosphoresistant mutants resemble the 103QHtt wt phenotype, the phosphomimic mutants showed homogeneous fluorescence in the cytosol, with a total absence of aggregates. Scale bar, 20 μm. **(B-E)** Quantitative analyses of microscopy pictures showed that the phosphoresistant mutation at Ser16 increases the percentage of cells with aggregates (B), but no significant differences were observed for the other parameters and phosphomutants. #, Significant versus non-mutated 103QHtt BiFC constructs, $p < 0.05$.

In order to measure the levels of oligomeric species and to determine the solubility of large aggregates, Native-PAGE immunoblotting and filter trap assays were performed (Figure 10). As previously described, 25QHtt wt forms single-size oligomeric species but not SDS-insoluble aggregates, and 103QHtt generates oligomeric species of variable size and large

insoluble aggregates (Herrera and Outeiro, 2012, Herrera et al., 2011). Cells transfected with phosphomimic mutants did not show SDS-insoluble aggregates in filter trap assays, confirming microscopy results (Figure 10, FT, top blots). The absence of SDS-insoluble aggregates was accompanied by an increase in the amount of oligomeric species in the case of the S16D mutant, but not in the T3D and S13D mutants (Figure 10, Native-PAGE). Interestingly, alanine amino acid substitution at Ser13 and Ser16 also led to a decrease in SDS-insoluble aggregates versus non-mutated 103QHtt. Alanine substitution at Thr3 did not have an effect on the production of SDS-insoluble aggregates. Unlike phosphomimic mutants, phosphoresistant BiFC pairs showed lower levels of oligomers and a more defined protein band.
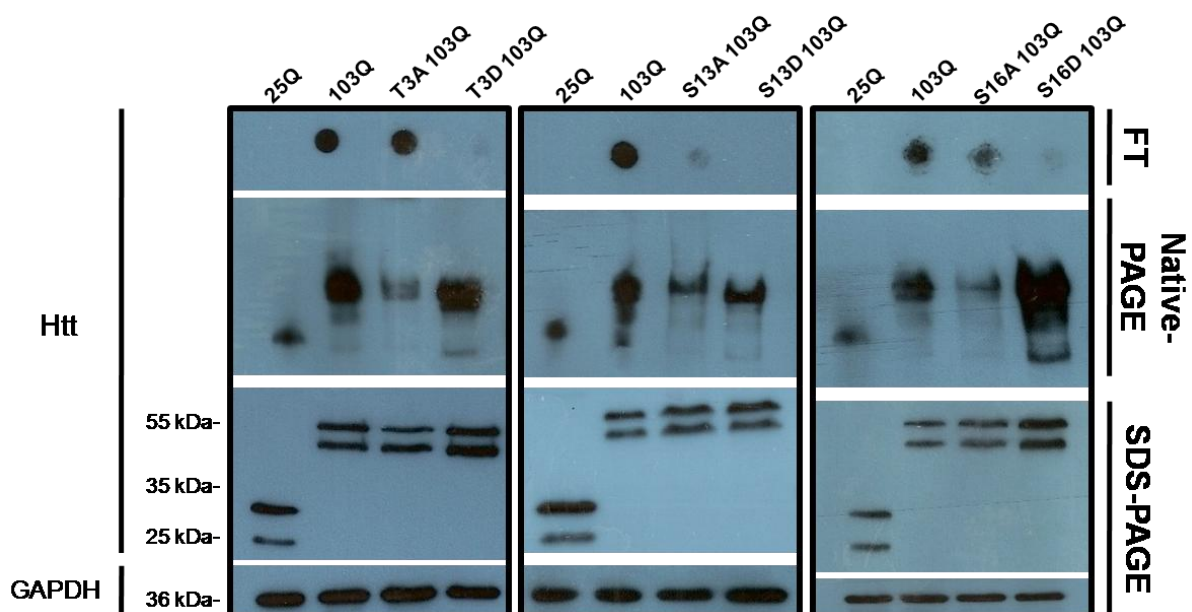
Figure 10. Phosphorylation of NT17 residues affects Htt oligomerization and the formation of large aggregates. Filter trap (FT) assays were consistent with microscopy results, showing that phosphomimic mutants do not produce SDS-insoluble aggregates. In the case of the S16D mutant, there is also a striking increase in the production of oligomeric species, as can be observed in native-PAGE conditions. Htt wt (25Q) did not produce SDS-insoluble aggregates or large amounts of oligomeric species. When transfected together

phosphomimic 103QHtt-V1 BiFC mutant and non-mutated 103QHtt-V2 BiFC constructs showed similar levels of SDS-insoluble aggregates but a mixed pattern in terms of oligomerization.

Although phosphomimic and phosphoresistant mutations resulted in different effects in terms of oligomerization as determined by Native-PAGE, flow cytometry analyses showed that both types of mutants had similar levels of fluorescence (Figure 11). Cells transfected with either phosphomimic or phosphoresistant mutants showed similar numbers of fluorescent cells versus non-mutated 103QHtt BiFC constructs, but a significantly increase in number of fluorescent cells when compared to 25QHtt wt BiFC constructs (Figure 11A-C). The reasons for the inconsistency between Native-PAGE and flow cytometry results are currently under study in our laboratory, and will be addressed in the Discussion section of the present thesis.

Taken together, these results suggest that the phosphorylation of the NT17 domain modulates mutant Htt aggregation and oligomerization.

A

B
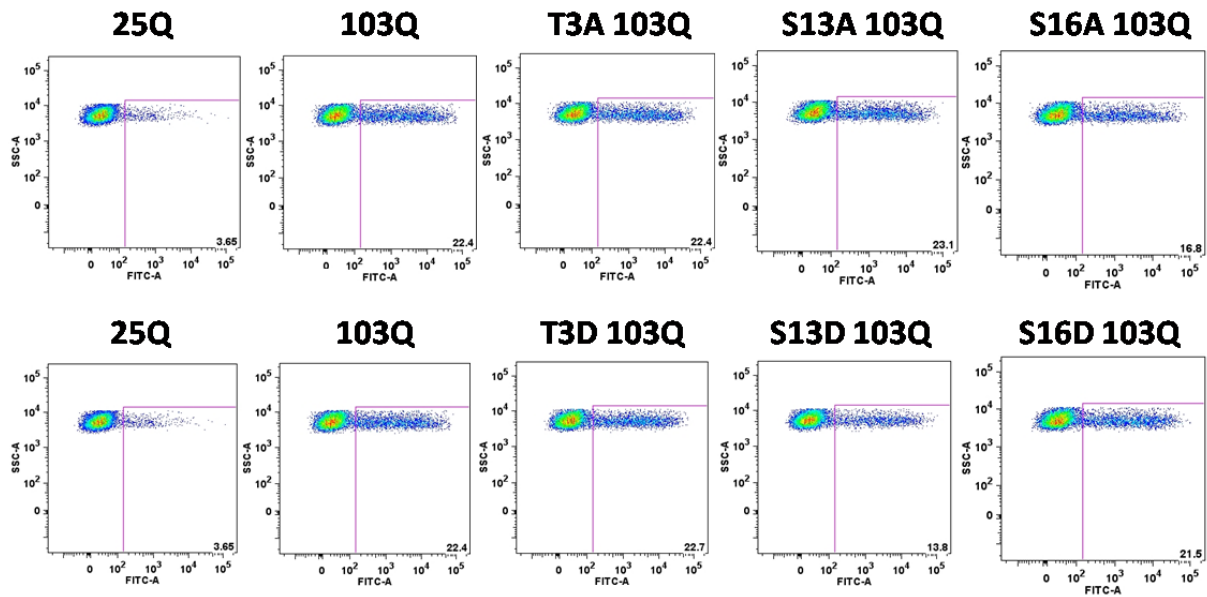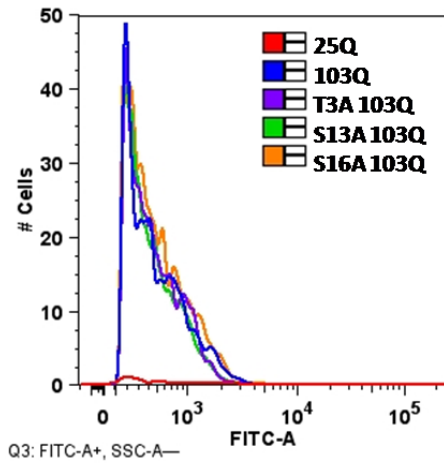
C

Figure 11. Phosphomimetic and phophoresistant mutations have no effect on fluorescence levels in H4 cells. (A) Cells transfected with phosphomimic or phophoresistant mutants showed similar number of

fluorescent cells comparing with non-mutant 103QHtt BiFC pair constructs, but an increase number of cells with fluorescence when compared with 25QHtt wt BiFC pair constructs. **(B)** Representative comparative histograms of flow cytometry analyses of the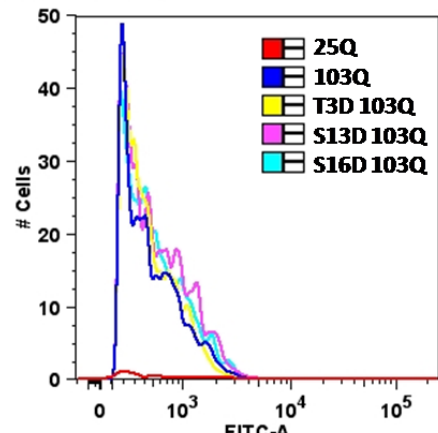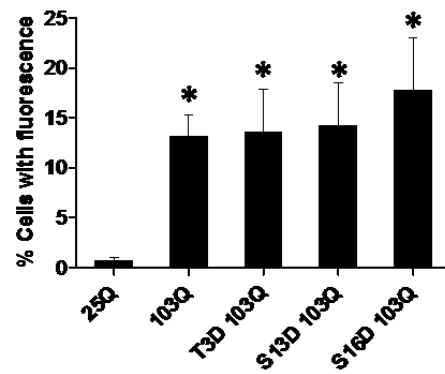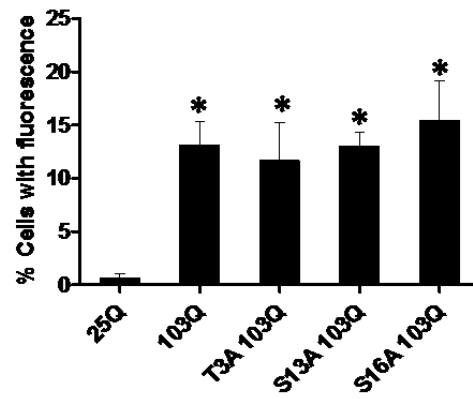 FL1 quadrant shown in A. **(C)** Graph showing the number of fluorescent cells in the different groups. *, Significant versus 25QHtt BiFC constructs, p<0.05.

4.2. Co-expression of phosphomimic mutants with non-mutated BiFC constructs recovers Htt aggregation pattern

In normal conditions the pool of Htt molecules would not be completely phosphorylated, but there would be a mixed population of phosphorylated and unphosphorylated Htt molecules. To further investigate the relationship between phosphorylated and unphosphorylated pools of Htt molecules both phosphomimic 103QHtt-Venus 1 plasmids and non-mutated 103QHtt-Venus 2 BiFC plasmids were co-transfected into H4 cells. The different combinations of plasmids showed a mixed phenotype in terms of aggregation (Figure 12). Most particularly, cells showed aggregates (Figure 12A), but in lower proportion than the non-mutant 103QHtt pair of constructs (Figure 12B). This indicates that phosphorylated Htt can still form aggregates in the presence of unphosphorylated Htt. The combination of 103QHtt T3D with non-mutant 103Q led to a marked decrease in the number of aggregates per cell (Figure 12C), but an increase in the percentage of aggregates larger than 3 μm (Figure 12E). This increase was also accompanied by a decrease in the proportion of aggregates smaller than 1μm (Figure 12E), suggesting that the T3D mutant promotes the aggregation of the smallest aggregates into larger aggregates when unphosphorylated Htt is present. Consistently, the expression of T3D mutants together with non-mutated Htt constructs also showed a total absence of cells with more than 25 aggregates, a significant decrease in the percentage of cells containing 10-25 aggregates and a significant increase in cells showing less than 10 aggregates (Figure 12D). On the other hand, co-transfection of S13D or S16D mutants and non-mutated constructs had no effect on the

number and size of aggregates (Figure 12C and 12E). However, the combination of S13D mutant with 103QHtt wt led to a lower percentage of cells showing 10-25 aggregates (Figure 12D).
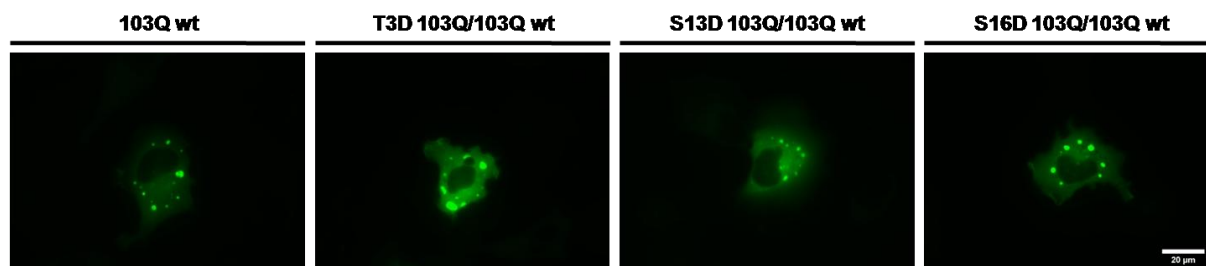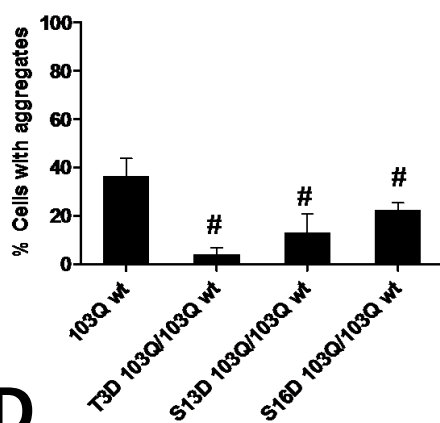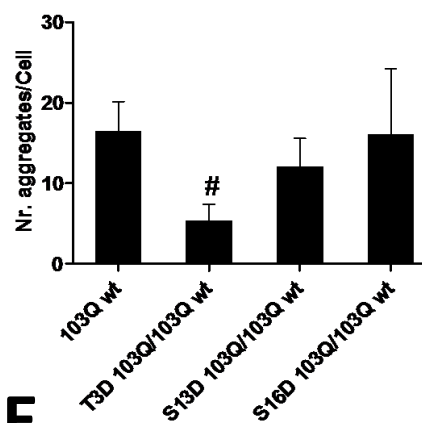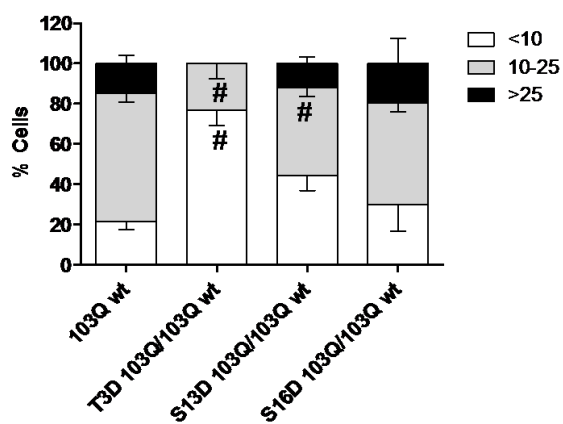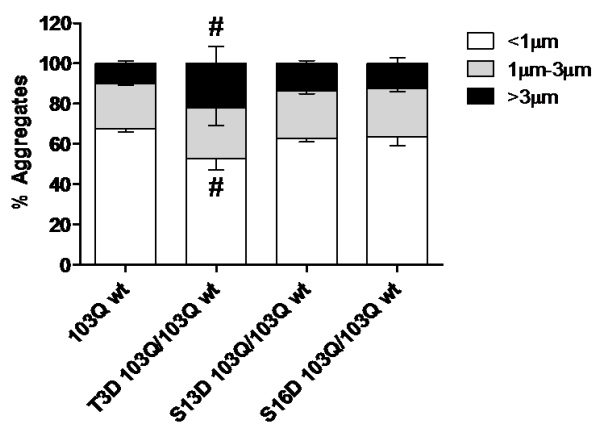
Figure 12. Co-expression of 103QHtt wt and phosphomimic mutants BiFC constructs recovers Htt aggregation pattern. **(A)** H4 cells were co-transfected with phosphomimic 103QHtt-Venus1 and non-mutated 103QHtt-Venus2 BiFC plasmids. These combinations showed mixed phenotypes in terms of aggregation. Scale bar, 20 μm. **(B-E)** Quantitative analyses of microscopy pictures for each combination of constructs. B, Percentage of cells that showed aggregates versus number of fluorescent (transfected) cells. C, Average number of aggregates per cell. D, Percentage of cells showing less than 10 aggregates, between 10 and 25 and more than 25, versus the total number of cells showing aggregates. E, Percentage of aggregates smaller than 1 μm, between 1 and 3 μm and larger than 3 μm, versus the total number of aggregates. #, Significant versus 103QHtt wt BiFC pair, $p < 0.05$.

Filter trap assays were consistent with microscopy results, showing that cells transfected with the different combinations of plasmids (phosphomimic 103QHtt-V1 mutants and non-mutated 103QHtt-V2) recovered the presence of SDS-insoluble aggregates (Figure 13). On the other hand, native-PAGE immunoblotting analyses showed a mixed oligomerization pattern. S13D or S16D 103Q / 103Q wt combinations produced higher amounts of oligomeric species, while T3D 103Q / 103Q wt combinations showed similar levels of oligomeric species than the 103QHtt wt pair of constructs. Again, flow cytometry analyses did not showed differences between the different combinations (Figure 14).

These results indicate that NT17 phosphorylation is a rate-limiting event in the balance between Htt oligomerization and aggregation in living cells. If the whole Htt pool is phosphorylated there are no aggregates and the balance shifts towards the production of oligomeric species. On the other hand, if there is a mixed population of molecules, the phosphorylation of the different NT17 residues produces different patterns of oligomerization and aggregation.
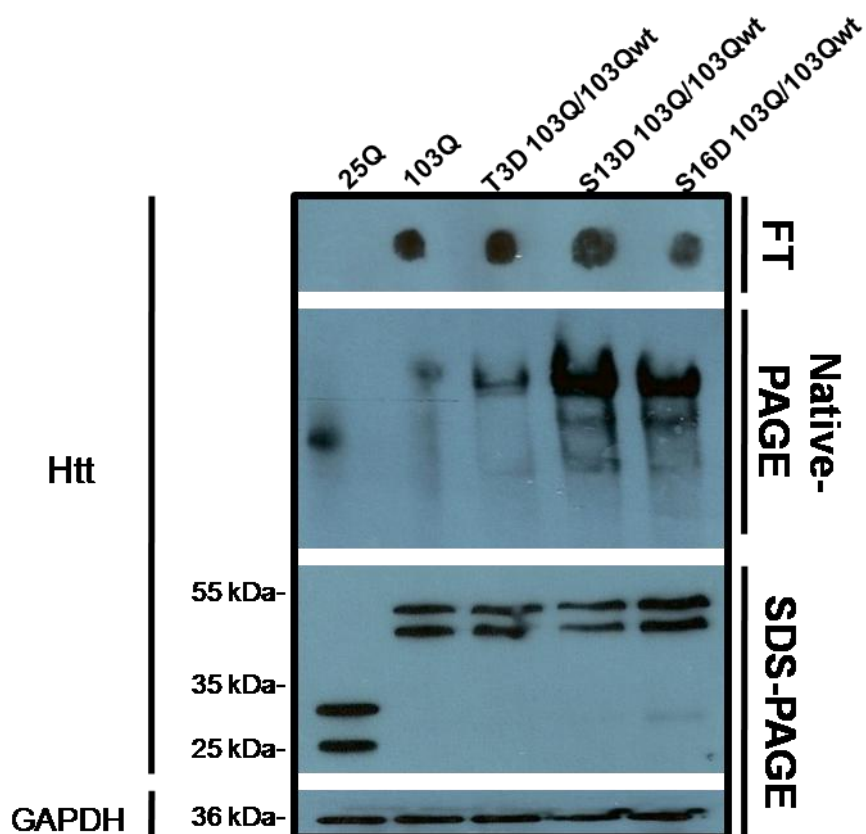
Figure 13. The combination of 103QHtt wt and phosphomimic mutants BiFC constructs results in different patterns of oligomerization. When transfected together, phosphomimic 103QHtt-V1 BiFC mutant and non-mutated 103QHtt-V2 BiFC constructs showed similar levels of SDS-insoluble aggregates but a mixed pattern in terms of oligomerization.
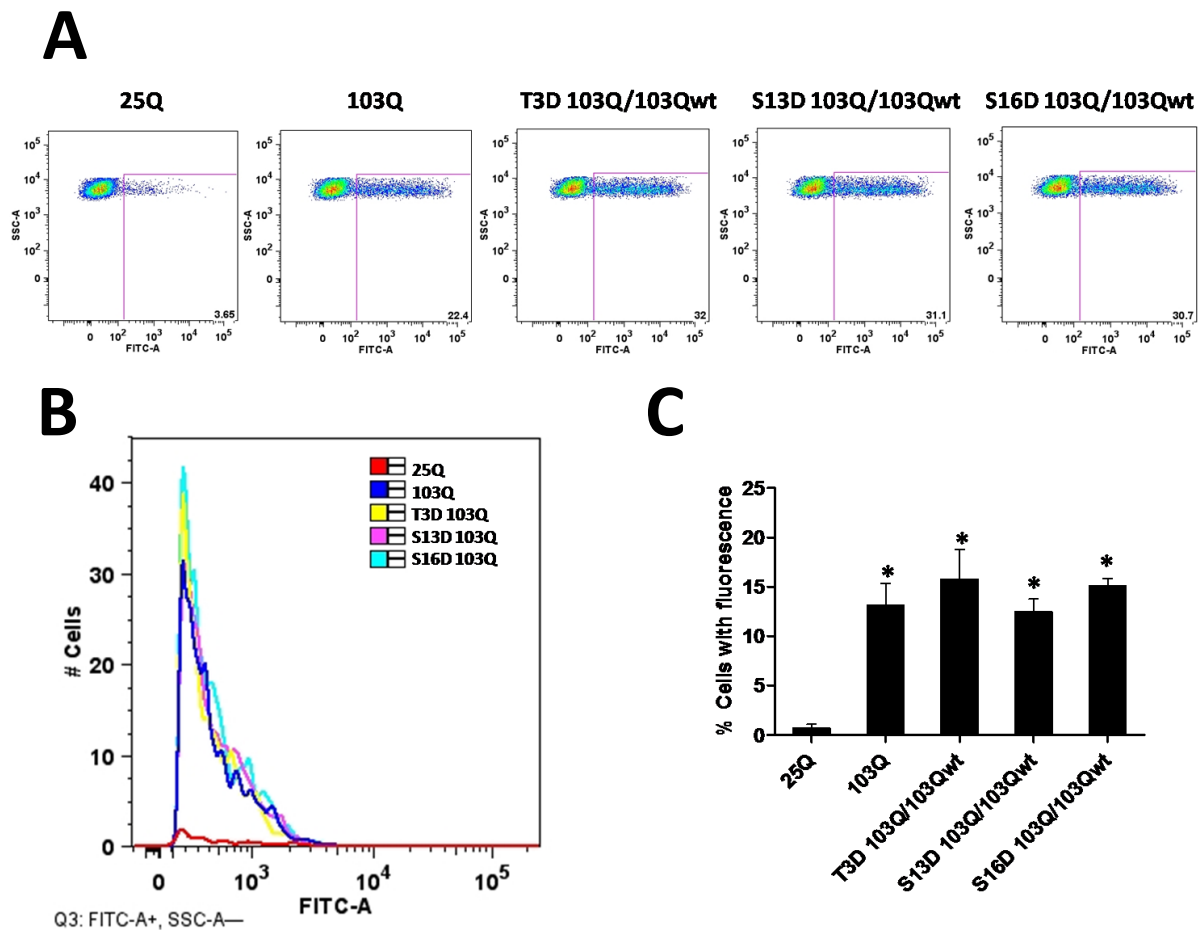
Figure 14. Co-transfection of 103QHtt wt BiFC constructs and phosphomimic mutants has no effect on fluorescence levels of H4 cells. (A, C) Cells were co-transfected with phosphomimic 103QHtt-Venus1 and non-mutated 103QHtt-Venus2 BiFC plasmids. These combinations showed similar number of fluorescent cells comparing with the 103QHtt wt BiFC pair, but an increased number of fluorescent cells when compared with the 25QHtt BiFC pair. **(B)** Representative histograms of flow cytometry analyses (from quadrant FL1 in A) showing equal levels of fluorescence between the different experimental groups.*, Significant versus 25QHtt BiFC pair, p<0.05.

4.3. Toxicity is not associated with Htt oligomerization or aggregation

Growing evidence indicates that the oligomeric soluble intermediates formed during aggregation process are the most toxic species (Arrasate et al., 2004, Bodner et al., 2006, Kuemmerle et al., 1999). Furthermore, phosphorylation pathways have been shown to modulate the toxicity of mutant Htt *in vitro* by affecting its aggregation dynamics (Atwal et al., 2011, Gu et al., 2009). In order to test whether phosphomimic or phosphoresistant

mutations had any effect in mutant Htt toxicity, LDH release assays were performed in H4 cells twenty-four hours after transfection (Figure 15). Either phosphoresistant or phosphomimic mutations at Thr3 did not modify mutant Htt toxicity (Figure 15A), while phosphoresistant mutations at Ser13 caused lower toxicity levels (Figure 15B). Both Ser16 phosphomutants showed a slight protective effect versus the non-mutated 103QHtt BiFC pair (Figure 15C). Interestingly, when 103QHtt wt and phosphomimic Htt BiFC constructs were combined, the toxicity was significantly decreased in all cases. The largest effect was obtained with the combination containing the S16D phosphomutant, which decreased mutant Htt toxicity to wt levels (Figure 15D).

These results are not correlated to the levels of Htt oligomeric species or aggregation. For example, the T3A phosphoresistant BiFC pair showed lower levels of oligomeric species (Figure 10), but did not decrease toxicity (Figure 15A). Conversely, while the S16D phosphomimic BiFC pair produced a striking increase in oligomeric species (Figure 10), it significantly prevented toxicity (Figure 15C). All phosphomimic pairs completely abolished the generation of large aggregates (Figure 9A). However, only the S16D pair prevented toxicity (Figure 15C). The combinations of 103QHtt wt and phosphomimic BiFC constructs produced diverse patterns of oligomerization and aggregation (Figure 12 and 13), but all of them prevented significantly toxicity (Figure 15D). Our results strongly suggest that there is not a direct association between Htt oligomerization, aggregation and toxicity.
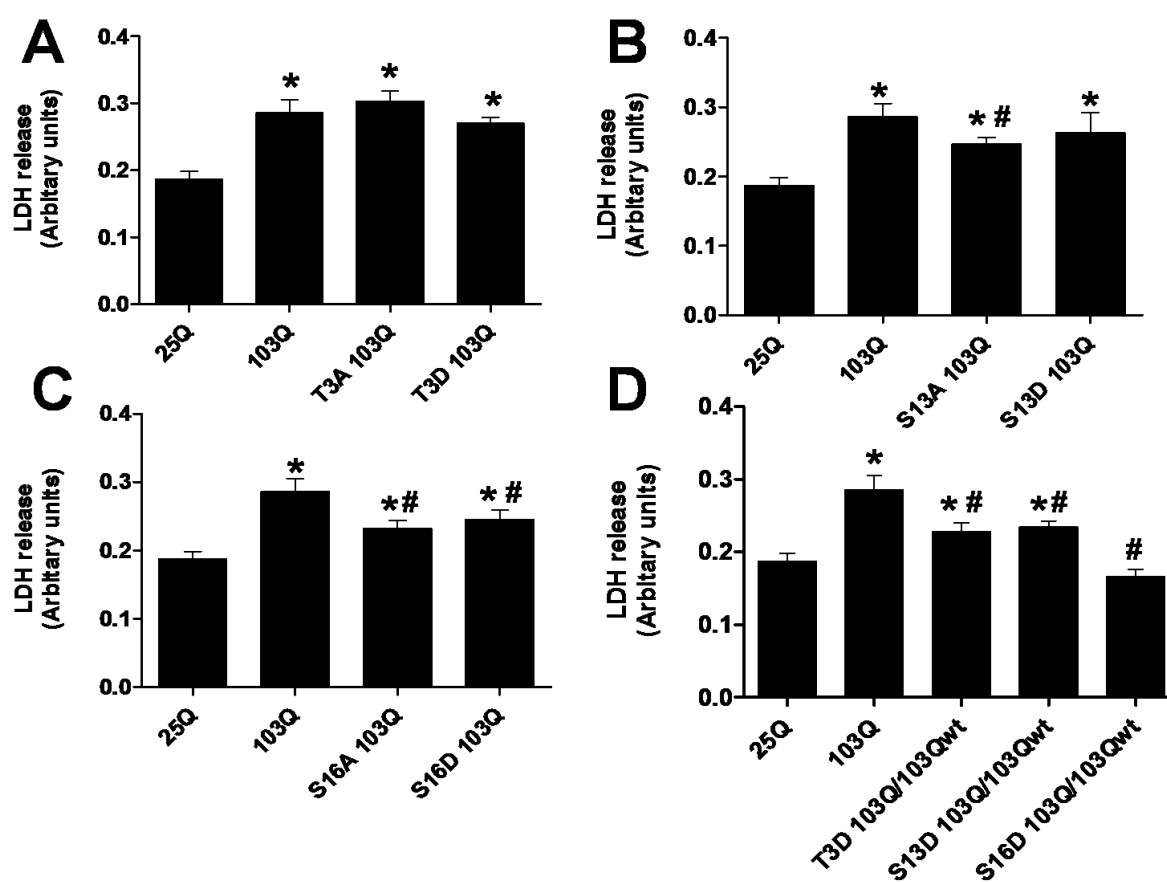
Figure 15. Toxicity is not associated with oligomerization or aggregation of Htt phosphomutants. (A) H4 cells were transfected with different combination of plasmids and cell toxicity was determined by LDH release assay. T3 phosphomutants did not modify the toxicity of mutant Htt. **(B)** Phosphoresistant, but not phosphomimetic mutations at Serine13 were significantly protective. **(C)** Both phosphoresistant and phosphomimetic mutations at Serine16 partially decrease toxicity. **(D)** Co-expression of phosphomimic mutants and single non-mutated 103QHtt BiFC constructs showed to be protective against mutant Htt toxicity, especially the S16 phosphomimic mutants, that decreases the toxicity to wild-type Htt levels. *Significant versus 25QHtt BiFC pair constructs, #Significant versus non-mutated 103QHtt BiFC pair constructs, p<0.05.

Table II. Summary of results

	BiFC constructs	Fluorescence	SDS-insoluble aggregates	Oligomeric species	Toxicity
Controls	25QHtt pair	+	-	+	-
	103QHtt pair	+++	+++	+++	+++
Phosphoresistant mutants	T3A 103QHtt pair	+++	+++	++	+++
	S13A 103QHtt pair	+++	++	++	++
	S16A 103Q Htt pair	+++	++	++	++
Phosphomimic mutants	T3D 103QHtt pair	+++	-	+++	+++
	S13D 103QHtt pair	+++	-	+++	+++
	S16D 103QHtt pair	+++	-	++++	++
Mixtures	T3D 103Q/103Q wt	+++	+++	+++	++
	S13D 103Q/103Q wt	+++	+++	++++	++
	S16D 103Q/103Q wt	+++	+++	++++	+

5. Discussion

In the present work, we showed that the phosphorylation of NT17 at any of its three phosphorylatable residues completely abolishes mutant Htt aggregation and alters its oligomerization pattern (Figure 9A and Figure 10, FT, top blots). Previous studies reported that amino acid substitution within the NT17 region alters the aggregation dynamics of mutant Htt, suggesting that the first 17 amino acids play a critical role in the intrinsic structure of the protein (Atwal et al., 2011, Gu et al., 2009, Mishra et al., 2012). Our results are consistent with the absence of large inclusions observed in the striatum and cortex of S13D/S16D phosphomimic HD mice (Gu et al., 2009). They also showed that double phosphoresistant or phosphomimic Ser13/Ser16 mutations confer distinct biophysical properties to the domain, changing its hydrophobicity and thereby affecting protein stability. Phosphoresistant serine-to-alanine substitutions increase the hydrophobicity of the residues and enhance the aggregation rate of Htt, whereas phosphomimic serine to aspartic acid substitutions decrease hydrophobicity and delays the aggregation process (Gu et al., 2009). Interestingly, the S16D mutant also show a striking increase in the amount of more soluble intermediate species (Figure 10, Native-PAGE), suggesting that the phosphorylation of this residue could redirect aggregation down a different assembly pathway. Previous kinetic studies showed that NT17 phosphorylation reduces fibrillization and causes the accumulation of intermediate aggregation products, resulting in both reduced aggregation kinetics and altered aggregate morphologies (Gu et al., 2009, Thakur et al., 2009).

The absence of large aggregates upon NT17 phosphorylation could also involve a greater activity of proteostasis mechanisms and molecular chaperones. This is supported by the fact that NT17 phosphorylation but not its desphosphorylation enhances the clearance of mutant Htt via lysosome-autophagy or ubiquitin-proteasome systems (Thompson et al., 2009).

Large intracellular aggregates are more common in the areas of the brain most affected by HD, such as the striatum. In HD-affected areas the levels of NT17 phosphorylation appear to be lower than in less compromised areas (Aiken et al., 2009). Moreover, the phosphorylation level is polyQ length-dependent, where longer polyQ tracts are associated with less phosphorylation, especially in HD-susceptible cells. These observations are consistent with our results and suggest that NT17 phosphorylation could be associated with a more efficient clearance of Htt aggregates.

In contrast to phosphomimic mutants, phosphoresistant mutants have a tendency to increase Htt aggregation (Figure 9A-D), which is consistent with previous *in vitro* reports (Atwal et al., 2011, Gu et al., 2009, Thakur et al., 2009). The aggregation-promoting effect of dephosphorylated Htt is further demonstrated by the fact that mixing phosphomimic mutants with non-mutated, expanded 103QHtt completely reversed the phosphomimic phenotype (Figures 12 and 13). This indicates that dephosphorylated Htt has a dominant, counteracting effect on phosphorylated Htt, promoting aggregation. However, filter trap results showed that S13A and S16A mutants had lower levels of SDS-insoluble aggregates when compared with their non-mutated counterpart, whereas T3A did not affect the production of insoluble Htt species (Figure 10, FT, top blots). Moreover, NT17 dephosphorylation induces a decrease in the levels of Htt soluble oligomeric species (Figure 10, Native-PAGE). These results suggest that the dephosphorylation of Ser13 or Ser16 maintains normal morphology of mutant Htt aggregates, but modifies the biophysical properties of Htt and probably their interaction with cellular components.

The analyses of oligomeric species by flow cytometry (Figures 11 and 14) and Native-PAGE (Figures 10 and 13, Native-PAGE) appeared to be inconsistent. In our model, fluorescence levels are expected to be directly proportional to the amount of oligomeric

species within cells. However, while phosphomutants showed similar fluorescence levels by flow cytometry (Figure 11), Native-PAGE immunoblots showed striking changes in the levels of oligomeric species in some of the phosphomutants (Figure 10, Native-PAGE). This inconsistency between the flow cytometry and the Native-PAGE results could be due to the particular features of the two different procedures. We have found two possible explanations for our results. First, while flow cytometry samples were whole cell cultures obtained with minimal processing, the immunoblotting samples were obtained from cell lysates, where the membranes are previously separated from the remaining cellular extract. The NT17 domain has a membrane binding signal that can modulate the association of Htt to the membranes of mitochondria, Golgi, endoplasmic reticulum, late endosomes and autophagic vesicles (Atwal et al., 2007, Rockabrand et al., 2007). Post-translational modifications of NT17 residues affect its subcellular localization and hydrophobicity. While mutations of threonine or serine residues to alanine would increase the hydrophobicity of Htt, inducing its association with membranes, mutations to aspartic acid would decrease hydrophobicity, inhibiting the association of Htt with membranes and increasing its levels in the aqueous fraction of the cytosol. Therefore, a considerable proportion of Htt could be attached to membranes and inside organelles, and discarded together with membrane pellets during protein isolation, in a way dependent of the hydrophobicity of each Htt version. This hypothesis would explain satisfactorily most filter trap and Native PAGE results, both the increase in oligomeric species shown in the S16D phosphomimic mutant and the decrease in insoluble aggregates (filter traps) and soluble oligomers shown in T3A, S13A and S16A phosphoresistant mutants. A second technical explanation is also possible. Flow cytometry results reflect the accumulated levels of dimers, but it is not able to discriminate if dimers further develop into oligomers or larger aggregates. In other words, flow cytometry is able to quantify the dimers that are

produced under particular conditions, but it does not provide qualitative information about how these dimers are associated. If this is true, then a decrease in large aggregates should be accompanied by an increase in oligomeric species, and viceversa. This is the case of S16D phosphomimic mutant and the mixtures of S13D or S16D phosphomimic mutants with non-mutated 103QHtt. Both hypotheses are plausible, and not necessarily mutually exclusive. We are currently carrying out further investigations in order to test them.

Our results strongly suggest that the effect of phosphomutants on Htt toxicity depends on the mutated residue and is not associated with the levels of oligomeric species or large inclusions. More particularly, although all phosphomimic mutants abolished the formation of large inclusions (Figure 9A), only the S16D mutation resulted in lower toxicity versus the 103QHttex1 BiFC pair (Figure 15). Additionally, both S16A and S16D mutant prevented toxicity (Figure 15) despite their clearly different oligomerization patterns (Figure 10). Currently there is still an intense debate about whether inclusion bodies are toxic or protective species. However, there is also a considerable body of evidence that these Htt species may represent epiphenomena, and that different mechanisms might be at play (Imarisio et al., 2008). Aberrant protein-protein interactions are thought to lie at the heart of cytotoxicity in the context of most neurodegenerative diseases (Goncalves et al., 2010). A few potential partners that could interact with the NT17 domain and modulate Htt toxicity have recently appeared (Omi et al., 2008, Wang et al., 2009). Additional post-translational modifications may also influence Htt toxicity. Phosphorylation at Ser13 by kinase IKK promotes acetylation and poly-SUMOylation of NT17 lysines. Post-translational modifications could therefore function together as a complicated compensatory mechanism to modulate Htt stability and toxicity (Thompson et al., 2009).

Our toxicity results are not totally consistent with previous studies showing that NT17 phosphorylation is associated with reduced toxicity (Atwal et al., 2011, Gu et al., 2009, Thompson et al., 2009). The substitution of the two NT17 serines by either aspartic acid (Gu et al., 2009, Thompson et al., 2009) or glutamic acid (Atwal et al., 2011) decrease the toxicity mediated by mutant Htt. These findings are consistent with our results, which showed a significantly reduced toxicity when the S16D mutation was present. However, when the phosphomimetic mutation to aspartic acid was produced only in Ser13, no effect on mutant Htt toxicity was observed. Bearing in mind previous studies using double serine phosphomimic mutants, our results suggest that the protective effect they observe could be mostly due to Ser16 phosphorylation. However, we cannot exclude that a double phosphorylation on Ser13 and Ser16 could enhance the effect of a single phosphorylation at Ser16. The effect of other double or triple phosphorylations of the three NT17 phosphorylatable residues should be further investigated.

We also demonstrated that both S13A and S16A phosphoresistant mutants led to a decrease in mutant Htt toxicity. In contrast, double mutations of NT17 serines to alanine were previously proven to not alter the toxicity of expanded Htt (Atwal et al., 2011, Thompson et al., 2009). This potential inconsistency could be explained by an accumulative effect of the double NT17 serine phosphomimic mutants that may lead to the neutralization of the protective effect produced when only one serine is mutated. Additionally, we showed that Thr3 mutants did not modify the toxicity of mutant Htt as opposed to previous results from Marsh and colleagues (Aiken et al., 2009). Aiken *et al*. (2009) showed that both phosphomimetic and phosphoresistant mutations at Thr3 prevent the lethality of a *Drosophila* HD model in approximately 50% versus flies carrying non-mutated 97QHtt and reduce Htt-mediated loss of eye photoreceptors. A possible explanation for these contradictory results

could be the different model organisms used. While they used an *in vivo* model and measured the photoreceptor cell death from *Drosophila's* eye, we used a neuroglioma cell line that provides a simpler and more stable microenvironment to better understand the role of NT17 phosphorylation at a cellular and molecular level. Moreover, our results suggest that, when a phosphorylated Htt molecule interacts with an unphosphorylated Htt molecule, toxicity is significantly reduced (Figure 15D). While there may be a fly homolog of human Htt, we were unable to observe Htt expression in our H4 cells. Therefore, the protective effect of Thr3 mutants in the *Drosophila* models could be due to their interaction with proteins that are not present in our cells, including Htt homologs, or to a different balance between phosphorylated and unphosphorylated pools of Htt. The effect of mixing phosphorylated and unphosphorylated pools on mutant Htt toxicity is independent of the residue, but is more remarkable when it concerns the Ser16 residue, suggesting a special role of this residue on the toxicity of expanded Htt.

In this work, we provide new insight about the relationship between phosphorylated and unphosphorylated pools of Htt molecules in living cells and how their interaction control Htt oligomerization, aggregation and toxicity. Furthermore, our results also contribute to the understanding of HD molecular and cellular pathogenic mechanisms, and to the development of future treatments for HD and other neurodegenerative disorders involving protein misfolding and aggregation.

6. Conclusions

In the present study, we provide evidence that:

1) Phosphorylation of the NT17 domain regulates the oligomerization, aggregation and toxicity of mutant Htt.

2) Dephosphorylated Htt molecules could have a dominant aggregation-promoting effect over phosphorylated Htt molecules.

3) The toxicity of mutant Htt is not clearly associated with its oligomerization or aggregation, indicating that other cellular or molecular mechanisms might be involved in Htt-mediated cell death.

Altogether, our results support the significance of NT17 phosphorylation in HD pathogenesis, and highlight the potential therapeutic value of targeting Thr3, Ser13 and Ser16 residues and the pathways that regulate their phosphorylation state. Further efforts should be made to elucidate the signaling pathways that modulate NT17 phosphorylation and to identify phosphorylation-dependent protein-protein interactions and post-translational modifications that regulate mutant Htt toxicity.

7. References

AGOROGIANNIS, E. I., AGOROGIANNIS, G. I., PAPADIMITRIOU, A. & HADJIGEORGIOU, G. M. 2004. Protein misfolding in neurodegenerative diseases. *Neuropathol Appl Neurobiol,* 30, 215-24.

AIKEN, C. T., STEFFAN, J. S., GUERRERO, C. M., KHASHWJI, H., LUKACSOVICH, T., SIMMONS, D., PURCELL, J. M., MENHAJI, K., ZHU, Y. Z., GREEN, K., LAFERLA, F., HUANG, L., THOMPSON, L. M. & MARSH, J. L. 2009. Phosphorylation of threonine 3: implications for Huntingtin aggregation and neurotoxicity. *J Biol Chem,* 284, 29427-36.

AMBROSE, C. M., DUYAO, M. P., BARNES, G., BATES, G. P., LIN, C. S., SRINIDHI, J., BAXENDALE, S., HUMMERICH, H., LEHRACH, H., ALTHERR, M. & ET AL. 1994. Structure and expression of the Huntington's disease gene: evidence against simple inactivation due to an expanded CAG repeat. *Somat Cell Mol Genet,* 20, 27-38.

ANNE, S. L., SAUDOU, F. & HUMBERT, S. 2007. Phosphorylation of huntingtin by cyclin-dependent kinase 5 is induced by DNA damage and regulates wild-type and mutant huntingtin toxicity in neurons. *J Neurosci,* 27, 7318-28.

ARRASATE, M., MITRA, S., SCHWEITZER, E. S., SEGAL, M. R. & FINKBEINER, S. 2004. Inclusion body formation reduces levels of mutant huntingtin and the risk of neuronal death. *Nature,* 431, 805-10.

ATWAL, R. S., DESMOND, C. R., CARON, N., MAIURI, T., XIA, J., SIPIONE, S. & TRUANT, R. 2011. Kinase inhibitors modulate huntingtin cell localization and toxicity. *Nat Chem Biol,* 7, 453-60.

ATWAL, R. S., XIA, J., PINCHEV, D., TAYLOR, J., EPAND, R. M. & TRUANT, R. 2007. Huntingtin has a membrane association signal that can modulate huntingtin aggregation, nuclear entry and toxicity. *Hum Mol Genet,* 16, 2600-15.

BATES, G. P., MANGIARINI, L. & DAVIES, S. W. 1998. Transgenic mice in the study of polyglutamine repeat expansion diseases. *Brain Pathol,* 8, 699-714.

BODNER, R. A., OUTEIRO, T. F., ALTMANN, S., MAXWELL, M. M., CHO, S. H., HYMAN, B. T., MCLEAN, P. J., YOUNG, A. B., HOUSMAN, D. E. & KAZANTSEV, A. G. 2006. Pharmacological promotion of inclusion formation: a therapeutic approach for Huntington's and Parkinson's diseases. *Proc Natl Acad Sci U S A,* 103, 4246-51.

BORRELL-PAGES, M., ZALA, D., HUMBERT, S. & SAUDOU, F. 2006. Huntington's disease: from huntingtin function and dysfunction to therapeutic strategies. *Cell Mol Life Sci,* 63, 2642-60.

CARMICHAEL, J., CHATELLIER, J., WOOLFSON, A., MILSTEIN, C., FERSHT, A. R. & RUBINSZTEIN, D. C. 2000. Bacterial and yeast chaperones reduce both aggregate formation and cell death in mammalian cell models of Huntington's disease. *Proc Natl Acad Sci U S A,* 97, 9701-5.

CHEN, C. D., OH, S. Y., HINMAN, J. D. & ABRAHAM, C. R. 2006. Visualization of APP dimerization and APP-Notch2 heterodimerization in living cells using bimolecular fluorescence complementation. *J Neurochem,* 97, 30-43.

CHUN, W., WALDO, G. S. & JOHNSON, G. V. 2011. Split GFP complementation assay for quantitative measurement of tau aggregation in situ. *Methods Mol Biol,* 670, 109-23.

CISBANI, G. & CICCHETTI, F. 2012. An in vitro perspective on the molecular mechanisms underlying mutant huntingtin protein toxicity. *Cell Death Dis,* 3, e382.

CORNETT, J., CAO, F., WANG, C. E., ROSS, C. A., BATES, G. P., LI, S. H. & LI, X. J. 2005. Polyglutamine expansion of huntingtin impairs its nuclear export. *Nat Genet,* 37, 198-204.

COSTA, M. C., MAGALHAES, P., FERREIRINHA, F., GUIMARAES, L., JANUARIO, C., GASPAR, I., LOUREIRO, L., VALE, J., GARRETT, C., REGATEIRO, F., MAGALHAES, M., SOUSA, A., MACIEL, P. & SEQUEIROS, J. 2003. Molecular diagnosis of Huntington disease in Portugal: implications for genetic counselling and clinical practice. *Eur J Hum Genet,* 11, 872-8.

DIFIGLIA, M., SAPP, E., CHASE, K. O., DAVIES, S. W., BATES, G. P., VONSATTEL, J. P. & ARONIN, N. 1997. Aggregation of huntingtin in neuronal intranuclear inclusions and dystrophic neurites in brain. *Science,* 277, 1990-3.

DUYAO, M., AMBROSE, C., MYERS, R., NOVELLETTO, A., PERSICHETTI, F., FRONTALI, M., FOLSTEIN, S., ROSS, C., FRANZ, M., ABBOTT, M. & ET AL. 1993. Trinucleotide repeat length instability and age of onset in Huntington's disease. *Nat Genet,* 4, 387-92.

DUYAO, M. P., AUERBACH, A. B., RYAN, A., PERSICHETTI, F., BARNES, G. T., MCNEIL, S. M., GE, P., VONSATTEL, J. P., GUSELLA, J. F., JOYNER, A. L. & ET AL. 1995. Inactivation of the mouse Huntington's disease gene homolog Hdh. *Science,* 269, 407-10.

EHRNHOEFER, D. E., SUTTON, L. & HAYDEN, M. R. 2011. Small changes, big impact: posttranslational modifications and function of huntingtin in Huntington disease. *Neuroscientist,* 17, 475-92.

FOROUD, T., GRAY, J., IVASHINA, J. & CONNEALLY, P. M. 1999. Differences in duration of Huntington's disease based on age at onset. *J Neurol Neurosurg Psychiatry,* 66, 52-6.

GAUTHIER, L. R., CHARRIN, B. C., BORRELL-PAGES, M., DOMPIERRE, J. P., RANGONE, H., CORDELIERES, F. P., DE MEY, J., MACDONALD, M. E., LESSMANN, V., HUMBERT, S. & SAUDOU, F. 2004. Huntingtin controls neurotrophic support and survival of neurons by enhancing BDNF vesicular transport along microtubules. *Cell,* 118, 127-38.

GHOSH, I., HAMILTON, A.D., REGAN, L. 2000. Antiparallel leucine zipper-directed protein reassembly: application to the green fluorescent protein. *J Am Chem Soc*, 122, 5658-5659.

GONCALVES, S. A., MATOS, J. E. & OUTEIRO, T. F. 2010. Zooming into protein oligomerization in neurodegeneration using BiFC. *Trends Biochem Sci,* 35, 643-51.

GU, X., GREINER, E. R., MISHRA, R., KODALI, R., OSMAND, A., FINKBEINER, S., STEFFAN, J. S., THOMPSON, L. M., WETZEL, R. & YANG, X. W. 2009. Serines 13 and 16 are critical determinants of full-length human mutant huntingtin induced disease pathogenesis in HD mice. *Neuron,* 64, 828-40.

HARTL, F. U. & HAYER-HARTL, M. 2009. Converging concepts of protein folding in vitro and in vivo. *Nat Struct Mol Biol,* 16, 574-81.

HAVEL, L. S., WANG, C. E., WADE, B., HUANG, B., LI, S. & LI, X. J. 2011. Preferential accumulation of N-terminal mutant huntingtin in the nuclei of striatal neurons is regulated by phosphorylation. *Hum Mol Genet,* 20, 1424-37.

HENG, M. Y., DETLOFF, P. J., WANG, P. L., TSIEN, J. Z. & ALBIN, R. L. 2009. In vivo evidence for NMDA receptor-mediated excitotoxicity in a murine genetic model of Huntington disease. *J Neurosci,* 29, 3200-5.

HERMEL, E., GAFNI, J., PROPP, S. S., LEAVITT, B. R., WELLINGTON, C. L., YOUNG, J. E., HACKAM, A. S., LOGVINOVA, A. V., PEEL, A. L., CHEN, S. F., HOOK, V., SINGARAJA, R., KRAJEWSKI, S., GOLDSMITH, P. C., ELLERBY, H. M., HAYDEN, M. R., BREDESEN, D. E. & ELLERBY, L. M. 2004. Specific caspase interactions and amplification are involved in selective neuronal vulnerability in Huntington's disease. *Cell Death Differ,* 11, 424-38.

HERRERA, F., GONCALVES, S. & OUTEIRO, T. F. 2012. Imaging protein oligomerization in neurodegeneration using bimolecular fluorescence complementation. *Methods Enzymol,* 506, 157-74.

HERRERA, F. & OUTEIRO, T. F. 2012. alpha-Synuclein modifies huntingtin aggregation in living cells. *FEBS Lett,* 586, 7-12.

HERRERA, F., TENREIRO, S., MILLER-FLEMING, L. & OUTEIRO, T. F. 2011. Visualization of cell-to-cell transmission of mutant huntingtin oligomers. *PLoS Curr,* 3, RRN1210.

HU, C. D., CHINENOV, Y. & KERPPOLA, T. K. 2002. Visualization of interactions among bZIP and Rel family proteins in living cells using bimolecular fluorescence complementation. *Mol Cell,* 9, 789-98.

HUMBERT, S., BRYSON, E. A., CORDELIERES, F. P., CONNORS, N. C., DATTA, S. R., FINKBEINER, S., GREENBERG, M. E. & SAUDOU, F. 2002. The IGF-1/Akt pathway is neuroprotective in Huntington's disease and involves Huntingtin phosphorylation by Akt. *Dev Cell,* 2, 831-7.

HUNTINGTON, G. 1872. On Chorea. *Medical and Surgical Reporter*, 26, 320–321.

IMARISIO, S., CARMICHAEL, J., KOROLCHUK, V., CHEN, C. W., SAIKI, S., ROSE, C., KRISHNA, G., DAVIES, J. E., TTOFI, E., UNDERWOOD, B. R. & RUBINSZTEIN, D. C. 2008. Huntington's disease: from pathology and genetics to potential therapies. *Biochem J,* 412, 191-209.

JANA, N. R., DIKSHIT, P., GOSWAMI, A., KOTLIAROVA, S., MURATA, S., TANAKA, K. & NUKINA, N. 2005. Co-chaperone CHIP associates with expanded polyglutamine protein and promotes their degradation by proteasomes. *J Biol Chem,* 280, 11635-40.

KAPLAN, A. & STOCKWELL, B. R. 2012. Therapeutic approaches to preventing cell death in Huntington disease. *Prog Neurobiol*.

KEGEL, K. B., MELONI, A. R., YI, Y., KIM, Y. J., DOYLE, E., CUIFFO, B. G., SAPP, E., WANG, Y., QIN, Z. H., CHEN, J. D., NEVINS, J. R., ARONIN, N. & DIFIGLIA, M. 2002. Huntingtin is present in the nucleus, interacts with the transcriptional corepressor C-terminal binding protein, and represses transcription. *J Biol Chem,* 277, 7466-76.

KERPPOLA, T. K. 2008. Bimolecular fluorescence complementation (BiFC) analysis as a probe of protein interactions in living cells. *Annu Rev Biophys,* 37, 465-87.

KROBITSCH, S. & KAZANTSEV, A. G. 2011. Huntington's disease: From molecular basis to therapeutic advances. *Int J Biochem Cell Biol,* 43, 20-4.

KUEMMERLE, S., GUTEKUNST, C. A., KLEIN, A. M., LI, X. J., LI, S. H., BEAL, M. F., HERSCH, S. M. & FERRANTE, R. J. 1999. Huntington aggregates may not predict neuronal death in Huntington's disease. *Ann Neurol,* 46, 842-9.

LAJOIE, P. & SNAPP, E. L. 2010. Formation and toxicity of soluble polyglutamine oligomers in living cells. *PLoS One,* 5, e15245.

LANDLES, C. & BATES, G. P. 2004. Huntingtin and the molecular pathogenesis of Huntington's disease. Fourth in molecular medicine review series. *EMBO Rep,* 5, 958-63.

LEAVITT, B. R., VAN RAAMSDONK, J. M., SHEHADEH, J., FERNANDES, H., MURPHY, Z., GRAHAM, R. K., WELLINGTON, C. L., RAYMOND, L. A. & HAYDEN, M. R. 2006. Wild-type huntingtin protects neurons from excitotoxicity. *J Neurochem,* 96, 1121-9.

LI, S. H. & LI, X. J. 1998. Aggregation of N-terminal huntingtin is dependent on the length of its glutamine repeats. *Hum Mol Genet,* 7, 777-82.

LUO, S. & RUBINSZTEIN, D. C. 2009. Huntingtin promotes cell survival by preventing Pak2 cleavage. *J Cell Sci,* 122, 875-85.

LUO, S., VACHER, C., DAVIES, J. E. & RUBINSZTEIN, D. C. 2005. Cdk5 phosphorylation of huntingtin reduces its cleavage by caspases: implications for mutant huntingtin toxicity. *J Cell Biol,* 169, 647-56.

MAAT-SCHIEMAN, M. L., DORSMAN, J. C., SMOOR, M. A., SIESLING, S., VAN DUINEN, S. G., VERSCHUUREN, J. J., DEN DUNNEN, J. T., VAN OMMEN, G. J. & ROOS, R. A. 1999. Distribution of inclusions in neuronal nuclei and dystrophic neurites in Huntington disease brain. *J Neuropathol Exp Neurol,* 58, 129-37.

MANGIARINI, L., SATHASIVAM, K., SELLER, M., COZENS, B., HARPER, A., HETHERINGTON, C., LAWTON, M., TROTTIER, Y., LEHRACH, H., DAVIES, S. W. & BATES, G. P. 1996. Exon 1 of the HD gene with an expanded CAG repeat is sufficient to cause a progressive neurological phenotype in transgenic mice. *Cell,* 87, 493-506.

MARTIN, B., GOLDEN, E., KESELMAN, A., STONE, M., MATTSON, M. P., EGAN, J. M. & MAUDSLEY, S. 2008. Therapeutic perspectives for the treatment of Huntington's disease: treating the whole body. *Histol Histopathol,* 23, 237-50.

MESTRE, T., FERREIRA, J., COELHO, M. M., ROSA, M. & SAMPAIO, C. 2009. Therapeutic interventions for disease progression in Huntington's disease. *Cochrane Database Syst Rev*, CD006455.

MISHRA, R., HOOP, C. L., KODALI, R., SAHOO, B., VAN DER WEL, P. C. & WETZEL, R. 2012. Serine Phosphorylation Suppresses Huntingtin Amyloid Accumulation by Altering Protein Aggregation Properties. *J Mol Biol*.

NASIR, J., FLORESCO, S. B., O'KUSKY, J. R., DIEWERT, V. M., RICHMAN, J. M., ZEISLER, J., BOROWSKI, A., MARTH, J. D., PHILLIPS, A. G. & HAYDEN, M. R. 1995. Targeted disruption of the Huntington's disease gene results in embryonic lethality and behavioral and morphological changes in heterozygotes. *Cell,* 81, 811-23.

NEVEKLOVSKA, M., CLABOUGH, E. B., STEFFAN, J. S. & ZEITLIN, S. O. 2012. Deletion of the huntingtin proline-rich region does not significantly affect normal huntingtin function in mice. *J Huntingtons Dis,* 1, 71-87.

NUCIFORA, F. C., JR., SASAKI, M., PETERS, M. F., HUANG, H., COOPER, J. K., YAMADA, M., TAKAHASHI, H., TSUJI, S., TRONCOSO, J., DAWSON, V. L., DAWSON, T. M. & ROSS, C. A. 2001. Interference by huntingtin and atrophin-1 with cbp-mediated transcription leading to cellular toxicity. *Science,* 291, 2423-8.

OMI, K., HACHIYA, N. S., TANAKA, M., TOKUNAGA, K. & KANEKO, K. 2008. 14-3-3zeta is indispensable for aggregate formation of polyglutamine-expanded huntingtin protein. *Neurosci Lett,* 431, 45-50.

ORR, A. L., LI, S., WANG, C. E., LI, H., WANG, J., RONG, J., XU, X., MASTROBERARDINO, P. G., GREENAMYRE, J. T. & LI, X. J. 2008. N-terminal mutant huntingtin associates with mitochondria and impairs mitochondrial trafficking. *J Neurosci,* 28, 2783-92.

OUTEIRO, T. F., PUTCHA, P., TETZLAFF, J. E., SPOELGEN, R., KOKER, M., CARVALHO, F., HYMAN, B. T. & MCLEAN, P. J. 2008. Formation of toxic oligomeric alpha-synuclein species in living cells. *PLoS One,* 3, e1867.

PANOV, A. V., GUTEKUNST, C. A., LEAVITT, B. R., HAYDEN, M. R., BURKE, J. R., STRITTMATTER, W. J. & GREENAMYRE, J. T. 2002. Early mitochondrial calcium defects in Huntington's disease are a direct effect of polyglutamines. *Nat Neurosci,* 5, 731-6.

PARDO, R., COLIN, E., REGULIER, E., AEBISCHER, P., DEGLON, N., HUMBERT, S. & SAUDOU, F. 2006. Inhibition of calcineurin by FK506 protects against polyglutamine-huntingtin toxicity through an increase of huntingtin phosphorylation at S421. *J Neurosci,* 26, 1635-45.

QIN, Z. H., WANG, Y., SAPP, E., CUIFFO, B., WANKER, E., HAYDEN, M. R., KEGEL, K. B., ARONIN, N. & DIFIGLIA, M. 2004. Huntingtin bodies sequester vesicle-associated proteins by a polyproline-dependent interaction. *J Neurosci,* 24, 269-81.

RANGONE, H., POIZAT, G., TRONCOSO, J., ROSS, C. A., MACDONALD, M. E., SAUDOU, F. & HUMBERT, S. 2004. The serum- and glucocorticoid-induced kinase SGK inhibits mutant huntingtin-induced toxicity by phosphorylating serine 421 of huntingtin. *Eur J Neurosci,* 19, 273-9.

RICHARDS, F. M. 1958. On the Enzymic Activity of Subtilisin-Modified Ribonuclease. *Proc Natl Acad Sci U S A,* 44, 162-6.

ROCHET, J. C. 2007. Novel therapeutic strategies for the treatment of protein-misfolding diseases. *Expert Rev Mol Med,* 9, 1-34.

ROCKABRAND, E., SLEPKO, N., PANTALONE, A., NUKALA, V. N., KAZANTSEV, A., MARSH, J. L., SULLIVAN, P. G., STEFFAN, J. S., SENSI, S. L. & THOMPSON, L. M. 2007. The first 17 amino acids of Huntingtin modulate its sub-cellular localization, aggregation and effects on calcium homeostasis. *Hum Mol Genet,* 16, 61-77.

ROOS, R. A. 2010. Huntington's disease: a clinical review. *Orphanet J Rare Dis,* 5, 40.

ROSS, C. A., WOOD, J. D., SCHILLING, G., PETERS, M. F., NUCIFORA, F. C., JR., COOPER, J. K., SHARP, A. H., MARGOLIS, R. L. & BORCHELT, D. R. 1999. Polyglutamine pathogenesis. *Philos Trans R Soc Lond B Biol Sci,* 354, 1005-11.

SAPP, E., SCHWARZ, C., CHASE, K., BHIDE, P. G., YOUNG, A. B., PENNEY, J., VONSATTEL, J. P., ARONIN, N. & DIFIGLIA, M. 1997. Huntingtin localization in brains of normal and Huntington's disease patients. *Ann Neurol,* 42, 604-12.

SHIN, J. Y., FANG, Z. H., YU, Z. X., WANG, C. E., LI, S. H. & LI, X. J. 2005. Expression of mutant huntingtin in glial cells contributes to neuronal excitotoxicity. *J Cell Biol,* 171, 1001-12.

SLOW, E. J., GRAHAM, R. K., OSMAND, A. P., DEVON, R. S., LU, G., DENG, Y., PEARSON, J., VAID, K., BISSADA, N., WETZEL, R., LEAVITT, B. R. & HAYDEN, M. R. 2005. Absence of behavioral abnormalities and neurodegeneration in vivo despite widespread neuronal huntingtin inclusions. *Proc Natl Acad Sci U S A,* 102, 11402-7.

SMITH, R., BRUNDIN, P. & LI, J. Y. 2005. Synaptic dysfunction in Huntington's disease: a new perspective. *Cell Mol Life Sci,* 62, 1901-12.

STEFFAN, J. S., AGRAWAL, N., PALLOS, J., ROCKABRAND, E., TROTMAN, L. C., SLEPKO, N., ILLES, K., LUKACSOVICH, T., ZHU, Y. Z., CATTANEO, E., PANDOLFI, P. P., THOMPSON, L. M. & MARSH, J. L. 2004. SUMO modification of Huntingtin and Huntington's disease pathology. *Science,* 304, 100-4.

STEFFAN, J. S., BODAI, L., PALLOS, J., POELMAN, M., MCCAMPBELL, A., APOSTOL, B. L., KAZANTSEV, A., SCHMIDT, E., ZHU, Y. Z., GREENWALD, M., KUROKAWA, R., HOUSMAN, D. E., JACKSON, G. R., MARSH, J. L. & THOMPSON, L. M. 2001. Histone deacetylase inhibitors arrest polyglutamine-dependent neurodegeneration in Drosophila. *Nature,* 413, 739-43.

STREHLOW, A. N., LI, J. Z. & MYERS, R. M. 2007. Wild-type huntingtin participates in protein trafficking between the Golgi and the extracellular space. *Hum Mol Genet,* 16, 391-409.

TAYLOR, J. P., HARDY, J. & FISCHBECK, K. H. 2002. Toxic proteins in neurodegenerative disease. *Science,* 296, 1991-5.

TELENIUS, H., KREMER, H. P., THEILMANN, J., ANDREW, S. E., ALMQVIST, E., ANVRET, M., GREENBERG, C., GREENBERG, J., LUCOTTE, G., SQUITIERI, F. & ET AL. 1993. Molecular analysis of juvenile Huntington disease: the major influence on (CAG)n repeat length is the sex of the affected parent. *Hum Mol Genet,* 2, 1535-40.

THAKUR, A. K., JAYARAMAN, M., MISHRA, R., THAKUR, M., CHELLGREN, V. M., BYEON, I. J., ANJUM, D. H., KODALI, R., CREAMER, T. P., CONWAY, J. F., GRONENBORN, A. M. & WETZEL, R. 2009. Polyglutamine disruption of the huntingtin exon 1 N terminus triggers a complex aggregation mechanism. *Nat Struct Mol Biol,* 16, 380-9.

THE HUNTINGTON'S DISEASE COLLABORATIVE RESEARCH GROUP, 1993. A novel gene containing a trinucleotide repeat that is expanded and unstable on Huntington's disease chromosomes. *Cell,* 72, 971–983.

THOMPSON, L. M., AIKEN, C. T., KALTENBACH, L. S., AGRAWAL, N., ILLES, K., KHOSHNAN, A., MARTINEZ-VINCENTE, M., ARRASATE, M., O'ROURKE, J. G., KHASHWJI, H., LUKACSOVICH, T., ZHU, Y. Z., LAU, A. L., MASSEY, A., HAYDEN, M. R., ZEITLIN, S. O., FINKBEINER, S., GREEN, K. N., LAFERLA, F. M., BATES, G., HUANG, L., PATTERSON, P. H., LO, D. C., CUERVO, A. M., MARSH, J. L. & STEFFAN, J. S. 2009. IKK phosphorylates Huntingtin and targets it for degradation by the proteasome and lysosome. *J Cell Biol,* 187, 1083-99.

TROTTIER, Y., BIANCALANA, V. & MANDEL, J. L. 1994. Instability of CAG repeats in Huntington's disease: relation to parental transmission and age of onset. *J Med Genet,* 31, 377-82.

TUKAMOTO, T., NUKINA, N., IDE, K. & KANAZAWA, I. 1997. Huntington's disease gene product, huntingtin, associates with microtubules in vitro. *Brain Res Mol Brain Res,* 51, 8-14.

VACHER, C., GARCIA-OROZ, L. & RUBINSZTEIN, D. C. 2005. Overexpression of yeast hsp104 reduces polyglutamine aggregation and prolongs survival of a transgenic mouse model of Huntington's disease. *Hum Mol Genet,* 14, 3425-33.

WANG, Y., LIN, F. & QIN, Z. H. 2010. The role of post-translational modifications of huntingtin in the pathogenesis of Huntington's disease. *Neurosci Bull,* 26, 153-62.

WANG, Y., MERIIN, A. B., ZAARUR, N., ROMANOVA, N. V., CHERNOFF, Y. O., COSTELLO, C. E. & SHERMAN, M. Y. 2009. Abnormal proteins can form aggresome in yeast: aggresome-targeting signals and components of the machinery. *FASEB J,* 23, 451-63.

WARBY, S. C., DOTY, C. N., GRAHAM, R. K., SHIVELY, J., SINGARAJA, R. R. & HAYDEN, M. R. 2009. Phosphorylation of huntingtin reduces the accumulation of its nuclear fragments. *Mol Cell Neurosci,* 40, 121-7.

WARRICK, J. M., CHAN, H. Y., GRAY-BOARD, G. L., CHAI, Y., PAULSON, H. L. & BONINI, N. M. 1999. Suppression of polyglutamine-mediated neurodegeneration in Drosophila by the molecular chaperone HSP70. *Nat Genet,* 23, 425-8.

WILLIAMSON, T. E., VITALIS, A., CRICK, S. L. & PAPPU, R. V. 2010. Modulation of polyglutamine conformations and dimer formation by the N-terminus of huntingtin. *J Mol Biol,* 396, 1295-309.

XIA, J., LEE, D. H., TAYLOR, J., VANDELFT, M. & TRUANT, R. 2003. Huntingtin contains a highly conserved nuclear export signal. *Hum Mol Genet,* 12, 1393-403.

YAMAMOTO, A., LUCAS, J. J. & HEN, R. 2000. Reversal of neuropathology and motor dysfunction in a conditional model of Huntington's disease. *Cell,* 101, 57-66.

YANG, D., WANG, C. E., ZHAO, B., LI, W., OUYANG, Z., LIU, Z., YANG, H., FAN, P., O'NEILL, A., GU, W., YI, H., LI, S., LAI, L. & LI, X. J. 2010. Expression of Huntington's disease protein results in apoptotic neurons in the brains of cloned transgenic pigs. *Hum Mol Genet,* 19, 3983-94.

ZEITLIN, S., LIU, J. P., CHAPMAN, D. L., PAPAIOANNOU, V. E. & EFSTRATIADIS, A. 1995. Increased apoptosis and early embryonic lethality in mice nullizygous for the Huntington's disease gene homologue. *Nat Genet,* 11, 155-63.

ZERON, M. M., CHEN, N., MOSHAVER, A., LEE, A. T., WELLINGTON, C. L., HAYDEN, M. R. & RAYMOND, L. A. 2001. Mutant huntingtin enhances excitotoxic cell death. *Mol Cell Neurosci,* 17, 41-53.

ZHENG, Z. & DIAMOND, M. I. 2012. Huntington disease and the huntingtin protein. *Prog Mol Biol Transl Sci,* 107, 189-214.

ZUCCATO, C., TARTARI, M., CROTTI, A., GOFFREDO, D., VALENZA, M., CONTI, L., CATAUDELLA, T., LEAVITT, B. R., HAYDEN, M. R., TIMMUSK, T., RIGAMONTI, D. & CATTANEO, E. 2003. Huntingtin interacts with REST/NRSF to modulate the transcription of NRSE-controlled neuronal genes. *Nat Genet,* 35, 76-83.

ZUCCATO, C., VALENZA, M. & CATTANEO, E. 2010. Molecular mechanisms and potential therapeutical targets in Huntington's disease. *Physiol Rev,* 90, 905-81.

ZUCCHELLI, S., MARCUZZI, F., CODRICH, M., AGOSTONI, E., VILOTTI, S., BIAGIOLI, M., PINTO, M., CARNEMOLLA, A., SANTORO, C., GUSTINCICH, S. & PERSICHETTI, F. 2011. Tumor necrosis factor receptor-associated factor 6 (TRAF6) associates with huntingtin protein and promotes its atypical ubiquitination to enhance aggregate formation. *J Biol Chem,* 286, 25108-17.